Journal of Coastal Research	17	3	563–583	West Palm Beach, Florida	Summer 2001

Pacific Storms, El Niño and Tsunamis: Competing Mechanisms for Sand Deposition in a Coastal Marsh, Euchre Creek, Oregon

Robert C. Witter,† Harvey M. Kelsey,‡ and Eileen Hemphill-Haley§

†William Lettis & Associates, Inc.
1777 Botelho Drive, Suite 262
Walnut Creek, CA 94596, U.S.A.

‡Department of Geology
Humboldt State University
Arcata, CA 95521, U.S.A.

§Department of Geological Sciences
1272 University of Oregon
Eugene, OR 97403, U.S.A.

ABSTRACT

WITTER, R.C.; KELSEY, H.M., and HEMPHILL-HALEY, E., 2001. Pacific storms, El Niño and tsunamis: competing mechanisms for sand deposition in a coastal marsh, Euchre Creek, Oregon. *Journal of Coastal Research,* 17(3), 563–583. West Palm Beach (Florida), ISSN 0749-0208.

During the past 600 years, 4 well-sorted sand beds, each with abrupt lower contacts, were deposited in the Euchre Creek marsh by storm waves and a tsunami. Brackish-marine diatoms preserved within the sand indicate a marine origin, but nonunique physical characteristics of the sand beds otherwise prevent the distinction of the depositional mechanism. However, a 150 year average recurrence interval for the sand beds is significantly smaller than the 500 to 540 year inferred recurrence interval for Cascadia subduction zone earthquakes, indicating that not all of the sand beds record local tsunamis. We consider storm-wave runup during extreme ocean levels and remote tsunamis generated elsewhere in the Pacific Rim, in addition to Cascadia tsunamis, as potential sand depositional mechanisms in washover settings of the Oregon coast. Magnitude-frequency analyses of tide gage and weather buoy data, along with historic records of remote tsunamis, indicate that storm-wave runup superimposed on extreme ocean levels attain heights >5 m every 10 years and may exceed 7 m every century, whereas remote tsunamis of similar magnitudes recur over periods of several hundred years. The best candidate for a tsunami deposit associated with the A.D. 1700 Cascadia earthquake is the thickest sand deposit which consists of multiple, fining-upward beds. The other sand deposits most likely record multiple episodes of storm-wave washover or possibly, but less likely, a remote tsunami. A simple model of relative sea-level response to the seismic cycle predicts that lower runup elevations were necessary for marine inundation of the marsh at times during the past 600 years due to coseismic subsidence.

ADDITIONAL INDEX WORDS: *Remote tsunami, storm-wave runup, magnitude-frequency analyses.*

INTRODUCTION

At least 27 historic tsunamis have attacked the Pacific coast of Oregon and northern California since 1854 (NGDC, 1998), yet these seismically-generated sea waves represent only one of several processes that generate extreme ocean levels and wave runup that can deposit sheets of marine-derived sand in coastal lakes and marshes. We consider three climatic and tectonic processes as candidate sand depositional mechanisms in washover settings: (1) storm-wave runup superimposed upon extreme ocean levels (the sum of high astronomical tides, storm surges and/or El Niño conditions), (2) local tsunamis generated by late Holocene earthquakes and sea-floor displacement in the accretionary prism of the Cascadia subduction zone, and (3) remote tsunamis generated by fault rupture and sea-floor displacement elsewhere in the Pacific Rim. Sand sheets containing marine microfossils preserved in stratigraphic sequences in washover-settings potentially record sedimentary response to tsunami inundation as well as climatic signals of El Niño and severe storms. However, the contribution of storms and El Niño to rates of sedimentation in Pacific Northwest coastal marshes is poorly understood.

Stratigraphic sequences beneath coastal marshes from southern Vancouver Island to northern California provide convincing evidence for tectonic deformation and accompanying tsunamis caused by prehistoric great (moment magnitude $M_w \geq 8$) earthquakes on the Cascadia subduction zone (ATWATER and HEMPHILL-HALEY, 1997; ATWATER *et al.,* 1995; CLAGUE and BOBROWSKY, 1994a; DARIENZO and PETERSON, 1990) (Figure 1). Widespread burial of marsh peat and forest soils, entombed by intertidal mud, serve as stratigraphic markers for episodes of coseismic subsidence (NELSON *et al.,* 1996b). Furthermore, anomalous sand beds sandwiched between mud-over-peat couplets are most commonly interpreted as deposits left by tsunamis that accompanied prehistoric great earthquakes (ATWATER and MOORE, 1992; BENSON *et al.,* 1997; CLAGUE and BOBROWSKY, 1994b; HEMPHILL-HALEY, 1995a; HUTCHINSON *et al.,* 1997; KELSEY *et al.,* 1998). Despite an apparent lack of historic seismicity on the Cascadia subduction zone, compelling geologic evidence suggests that prehistoric great earthquakes may recur, on average, as often as 500 to 540 years and pose seismic and tsunami hazards to Pacific Northwest coastal communities (ATWATER and HEMPHILL-HALEY, 1997).

99116 received 13 December 1999; accepted in revision 12 February 2001.

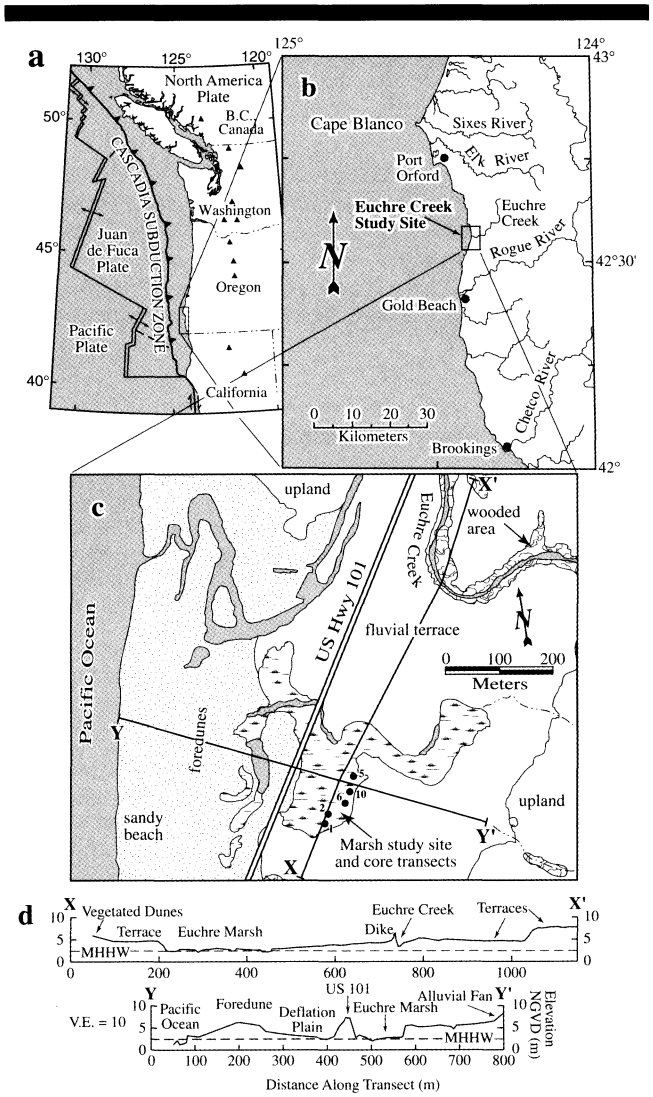

Figure 1. (a) Location of Euchre Creek with respect to the Cascadia convergent margin of the Pacific Northwest, U.S.A., triangles denote volcanoes of the Cascade arc. (b) Regional map of southern coastal Oregon showing location of Euchre Creek study site, 23 km south of Port Orford. (c) Map of the freshwater marsh at Euchre Creek, south coastal Oregon. Closed circles show the locations of selected cores within the marsh. The average elevation of the marsh is 1.8 m above mean higher high water (MHHW), based on surveys tied to a tide gauge at Port Orford 23 km to the north. The highest observed water level at Port Orford during the period from 1979 to 1990 (NOS, 1992) reached to within ~0.4 m below the lowest surface of the Euchre Creek marsh. (d) Topographic profiles of transects X-X′ and Y-Y′ in Figure 1a. Dashed line on the profiles shows relative elevation of MHHW.

Without accompanying evidence of subsidence and shaking, sheets of tsunami derived sand in marsh stratigraphic sequences are difficult to distinguish from sand beds deposited by nonseismic coastal processes that generate extreme ocean levels such as the combined effects of storm surges, storm-wave runup and El Niño events (NELSON *et al.*, 1996b). The most recent earthquake or series of earthquakes caused coseismic subsidence over 900 km of coastline about 300 years ago based on radiocarbon ages of earthquake-killed plants from the youngest buried marsh soil at nine Pacific Northwest marshes (NELSON *et al.*, 1995). In addition, on the basis of Japanese tsunami records of January 1700, this earthquake generated a tsunami that propagated westward across the Pacific Ocean (SATAKE *et al.*, 1996). Geologic evidence for an Oregon tsunami 300 years ago caused by this earthquake consists of sand sheets that overlie abruptly buried marsh soils and exhibit biostratigraphic evidence of a marine source; the sand sheets thin landward and are coincident with evidence for coseismic subsidence and seismic shaking (ATWATER *et al.*, 1995).

The objective of this paper is to demonstrate that extreme ocean levels caused by climatological phenomena are more frequent than remote tsunamis of similar magnitude and therefore represent the most plausible mechanisms, in addition to Cascadia tsunamis, for sand deposition in Oregon coastal environments. Understanding the different frequencies of climatic and tectonic processes likely to deposit sand in coastal marshes will aid in the interpretation of marsh stratigraphic sequences containing interbedded peat, mud and sand. However, because sand beds deposited by tsunamis and sand beds deposited during storms cannot unequivocally be distinguished on the basis of lithological characteristics, and because extreme ocean levels and storm waves may attain sufficient elevations to deposit sand in washover settings every decade, the frequency of tsunami deposits in the geologic record may be overestimated. Therefore, given the 500 to 540 yr recurrence interval for great earthquakes recorded at Willapa Bay, Washington (ATWATER and HEMPHILL-HALEY, 1997), and assuming each earthquake generated a local tsunami that could transport and deposit sand in washover environments, we would attribute no more than 1 to 2 sand beds to local tsunamis for every 500 to 540 years of marsh aggradation. Because the marsh at Euchre Creek (Figure 1b) harbors evidence for four episodes of sand deposition in the last 600 years, we posit that mechanisms other than local tsunamis introduced sand into the marsh. This paper provides an analysis of the frequency and magnitude of processes other than local tsunamis that could deposit sand beds in a coastal Oregon marsh.

WASHOVER SETTINGS SUSCEPTIBLE TO SAND DEPOSITION BY EPISODES OF EXTREME OCEAN LEVELS

A wide range of coastal settings in Oregon are susceptible to marine inundation during storms as well as inundation by tsunami. A simple, end-member model of a depositional setting likely to record tsunamis and storm-wave runup during extreme ocean levels is the washover setting (Figure 2). Depositional environments in washover settings on the Oregon coast include lagoons, lakes and marshes <5 m above the National Geodetic Vertical Datum, that are protected from the open ocean by a single sand barrier or dune field. Lakes and lagoons form when migrating dunes or wave-transported sand block the outlets of small coastal streams and creeks. In some cases the sand barriers that contain these fresh-to-brackish water bodies are breached either by storm waves or by high stream flow during late fall/early winter floods, demonstrating the ephemeral na-

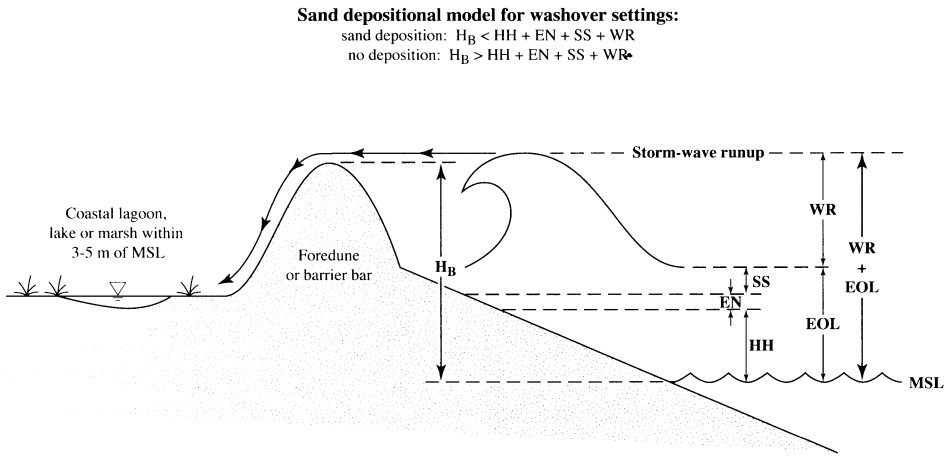

Figure 2. Sand deposition model for washover settings susceptible to tsunamis and storm-wave runup during extreme ocean levels. Deposition of sand may occurs when extreme ocean levels (EOL), equal to the sum of astronomical tide (HH), storm surge (SS) and El Niño (EN) conditions, plus storm-wave runup (WR) exceed the height of the dune or sand barrier (H_B). Storm-wave runup plus extreme ocean levels that do not exceed the height of the barrier do not deposit sand layers in washover settings. However, repeated wave attack may cause erosion severe enough to significantly erode or breach the sand barrier, thus lowering the effective runup height necessary for inundation. MSL, mean sea level, is approximately equal to NGVD at most Oregon tide gages (modified from Figure 1 of SHIH and KOMAR, 1994).

ture of these lagoons and their susceptibility to marine inundation. Marshes in deflation plains and within barrier embayments in Oregon estuaries also represent washover settings that can potentially preserve sand beds deposited by tsunamis and extreme climatic events. Although more complicated than the simple model shown in Figure 2, the Euchre Creek marsh (Figure 1c) exemplifies a washover site where we investigated a stratigraphic sequence containing four sand beds that may record multiple depositional mechanisms including tsunamis and storm-wave runup.

In coastal lagoons and lakes, or in freshwater marshes that lack brackish/marine diatom assemblages necessary for estimating magnitudes of sudden relative sea-level rise indicative of subsidence, interbedded sand beds may record flooding, eolian transport, storm waves or tsunami (BENSON *et al.*, 1997; HUTCHINSON *et al.*, 1997; NELSON *et al.*, 1996b; SHENNAN *et al.*, 1998). Flood deposits generally thicken and coarsen inland and are distinguished from marine deposits because they commonly contain freshwater diatom assemblages. In contrast, wind transported sand from barrier sand spits and dune fields, which commonly comprise the seaward border of coastal lakes and marshes, are typically barren of microfossils owing to winnowing effects. Marine-derived sand beds deposited by storm waves and tsunamis contain brackish/marine microfossil assemblages indicating a transport direction from the sea. In terms of sedimentary structure, storm waves that overtop sand barriers leave inversely graded, laminated overwash deposits (SALLENGER, 1979; LEATHERMAN *et al.*, 1977; SCHWARTZ, 1975) similar to the texture and grading observed in the upper swash zone of beaches (CLIFTON, 1969).

Several researchers who have made stratigraphic investigations of Pacific Northwest salt marshes interpret sand beds interbedded with abruptly buried soils and overlying intertidal mud as the deposits of local tsunamis generated by rupture of the Cascadia subduction zone (ATWATER and MOORE, 1992; BENSON *et al.*, 1997; CLAGUE and BOBROWSKY, 1994b; DARIENZO and PETERSON, 1990; HEMPHILL-HALEY, 1995). The physical characteristics of tsunami deposits consist of fining-upward sheets of landward-thinning sand and gravel, which, in some cases, occur as multiple beds reflecting multiple tsunami waves (ATWATER and MOORE, 1992; SATO *et al.*, 1995). Sand beds preserved concurrently with stratigraphic evidence for coseismic subsidence may record local tsunamis generated on the Cascadia subduction zone. However, in most cases sand beds do not exhibit clear lithological characteristics that indicate whether the sand was deposited by storm waves or a tsunami (FOSTER *et al.*, 1991; SATO *et al.*, 1995). Finally, little is understood about the nature and frequency of storm-generated deposits preserved beneath Oregon marshes, or the contribution of this process to rates of marsh sedimentation (*e.g.*, REJMÁNIK *et al.*, 1988).

Sand deposition and severe erosion during coastal storms is well studied in the southeastern U.S. and Hawaii where tropical storms and hurricanes can produce storm surges exceeding 6 m (COCH, 1994). Historically, hurricanes do not occur on the Oregon coast, but severe winter storms can compare in duration and wind velocity to extratropical storms in the Gulf of Mexico. For example, GOODBRED and HINE (1995) investigated storm surge deposits in Waccasassa Bay, Florida due to the "Storm of the Century," an extratropical storm that developed in March 1993 in the Gulf of Mexico. During this storm onshore winds >15.4 m/s persisted for 16 hours, with gusts exceeding 41 m/s, and drove a storm surge >2.5 m in height into coastal salt marshes resulting in a 12-cm-thick sandy storm deposit. For comparison, during a severe storm at Newport, Oregon over December 14 to 16, 1997, the National Data Buoy Center climate buoy at Yaquina Bay (NDBC, 1998) recorded wind velocities >15.0 m/s persisting for 16 hours with gusts reaching 25 m/s (Figure 3). This storm produced a surge between 0.5 to 0.6 m

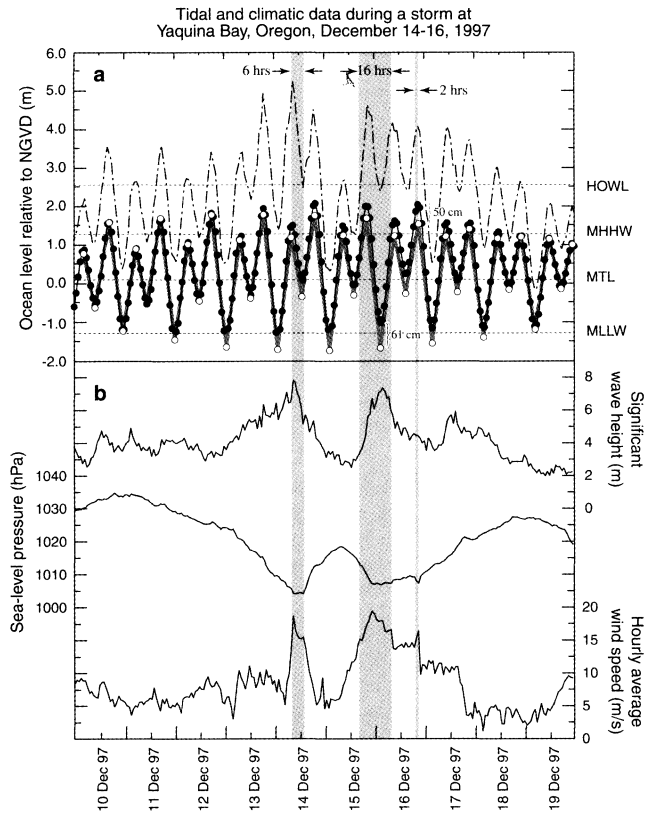

Figure 3. Extreme ocean level plus wave runup, tidal stage, wind velocity, sea-level pressure, and significant wave height observed during a severe storm at Yaquina Bay, December 10 to 19, 1997. (a) Open circles connected by broad grey line denote predicted tide levels; closed circles connected by thin black line denote measured tide elevations based on the Yaquina Bay tide gage (NOS, 1992). Vertical grey bands indicate duration of hours when peak wind velocity exceeded 15 m/s and correspond to periods of highest storm surge. For example, ocean setup caused by a storm surge 0.5 to 0.6 m in height resulted from persistent wind velocities >15.0 m/s for over 16 hours coinciding with low sea-level pressures. The dashed line estimates the highest elevation marine waters may have attained during the December 1997 storm as a result of storm-wave runup superimposed on extreme ocean level (measured tide). The sum of storm-wave runup, predicted for the observed significant wave height (Equation 1), and measured tide level exceeded 4 m during 7 periods over the course of the storm. On one occasion, during the low-high tide (1.5 m) on December 14, 1997, the wave runup estimate exceeded 3.7 m; thus, the combination of extreme ocean level plus storm-wave runup around 9 AM on December 14, 1997 may have reached 5.2 m above NGVD. (b) Significant wave height, sea-level pressure and wind velocity observed simultaneously at one hour intervals by the Yaquina Bay climate buoy (NDBC, 1998).

at the Newport tide gage and also caused extreme ocean levels in British Columbia indicating the regional impact of this event. In March 1999 at Willapa Bay, Washington the measured tide exceeded the predicted tide by more than 1.7 m recording an exceptional storm surge during a more recent intense Pacific storm (KOMAR *et al.,* in press). The magnitude of the storm surges produced in Oregon are probably less than those generated by Gulf storms because the slope of the continental shelf offshore Oregon is greater than the gently sloping shelf in the Gulf, and southerly storm winds in Oregon approach the coast obliquely rather than orthogonally. However, inundation by storm-wave runup superimposed on top of extreme ocean levels during Pacific Northwest storms may exceed 5 m every decade (RUGGIERO *et al.,* 1996) and possibly exceed 7 m every century (KOMAR *et al.,* in press).

There are only a few coastal investigations in the Pacific Northwest that conclude sand deposition in washover settings arose from storm waves and extreme ocean levels. Storm-wave washover during the El Niño winter of 1997–98 caused sand deposition at two locations in Oregon. Near Port Orford, 23 km north of Euchre Creek (Figure 1b), severe storm-wave erosion of a sewage treatment drain field and the beach/dune barrier of Garrison Lake allowed storm waves to transport sand from the beach and deposit it into the lake (KOMAR, 1998). Storm waves superimposed on extreme ocean levels also resulted in washover at Cape Lookout State Park, south of Netarts Bay, depositing sand in the park campground (KOMAR, 1998). Much greater washover occurred at Cape Lookout during the 1998–99 winter (P. KOMAR, pers. comm., 2000). In a separate investigation, SHENNAN *et al.* (1998) reconstructed the evolution of Netarts Bay to test whether the subduction zone earthquake deformation cycle explained the presence of mud-over-peat couplets in stratigraphic sequences previously studied by DARIENZO and PETERSON (1990) and DARIENZO *et al.* (1994). Netarts Bay, protected from the open ocean by a ~9 km long, narrow sand spit, represents a washover setting that may be susceptible to extreme ocean levels and storm-wave runup. Based on pollen and diatom analyses, they concluded that a 0.5 cm sand layer overlying a mud-over-peat couplet from the lower part of core NB-2 recorded sedimentation in the marsh that reflected small-order (<0.5 m) oscillations in relative sea level brought about by nonseismic changes in the hydrography of the estuary (SHENNAN *et al.,* 1998). Considering the extreme nature of the storm climate of the Oregon coast, it remains plausible that sand beds lacking sufficient evidence for deposition accompanied by coseismic subsidence may have been deposited during intense coastal storms, not tsunamis.

In the following section we present estimates, summarized in Table 1, of recurrence intervals and magnitudes for climatic and tectonic processes that we consider as candidate sand depositional mechanisms on the Oregon coast. When evaluating the magnitude of storm-wave runup for extreme events, multiple atmospheric and oceanic processes must be considered. Some of these processes occur independently, whereas others occur at the same time. As a result, the joint probability of occurrence for two independent processes—for example, a storm surge during a perigean Spring tide—would be less than the joint probability of two dependent processes like storm waves elevated by a storm surge. Unless otherwise noted, all tidal and land elevations presented in this paper refer to the U.S. National Geodetic Vertical Datum (NGVD) of 1929.

MAGNITUDE-FREQUENCY RELATIONS OF CLIMATIC PHENOMENA VERSUS TSUNAMIS

Extreme ocean levels on the Oregon coast result from the joint occurrence of storm surges during eastern Pacific storms and high water levels produced by exceptional astronomical tides or

El Niño events. This section will discuss reported sea-level anomalies due to storm surges in the Pacific Northwest as determined by differencing the measured tide level from the predicted tide level during severe Pacific storms. This section also will present storm wave runup elevations predicted by sea cliff and dune erosion models, an analysis of runup heights for remote tsunamis and the expected runup height for a local tsunami generated by offshore displacement of the Cascadia subduction zone.

Anomalous Sea Levels Owing to El Niño

During the 1982–83 and 1997–98 El Niños anomalous monthly mean sea levels exceeded normal winter mean sea levels by 0.35 to 0.4 cm (HUYER *et al.*, 1983) and resulted in severe erosion on the Oregon coast (KOMAR, 1986; KOMAR, in press). WYRTKI (1975) demonstrated that the meteorological and oceanographic effects of El Niño result from a relaxation of southeast equatorial trade winds which leads to the collapse and westward propagation of high-standing western Pacific equatorial water. Upon reaching South America, the resulting pulse of warm water splits into two sea-level waves that migrate to the north and south. Trapped by the Coriolis force, the northern sea-level bulge refracts across the continental slopes of North and South America and hugs the coastline as it propagates 75 km/day northward (KOMAR, 1986). The warmer mean ocean temperature and strong currents associated with the sea-level bulge results in a persistent increase in mean tide levels up to 0.5 m (KOMAR, 1986).

Long term variations in El Niño frequency patterns since A.D. 622 appear to be linked to variations in solar activity (DIAZ and MARKGRAF, 1992). Based on Nile flood records and historical records of El Niño events, the mean recurrence interval over the past ~1400 years is ~4 years. For our purposes a slightly longer period of 7 to 8 years for strong and very strong El Niño events is probably a more accurate estimate of the frequency of events likely to cause significant 0.3 to 0.5 m anomalies in sea level for Oregon. However, it is important to note that the long term frequency for more severe events also has varied over the past millennium, thus recurrence intervals for El Niño events in the late Holocene may have ranged from 7 to 30 years (DIAZ and MARKGRAF, 1992). Higher mean sea levels caused by these events are alone insufficient to inundate low lying coastal areas and deposit sand. It is the combined effect of elevated sea level during El Niño plus the surge and wave runup generated during Oregon storms that can reach sufficiently high elevations to deposit sand in coastal marshes.

The joint occurrence of a major storm surge during El Niño years must be considered a random event involving two independent processes. For example, high monthly mean water levels attributed to El Niño result from warmer water temperatures and strong ocean currents, factors that are independent from windshear during severe storms that generates storm surges (KOMAR and ALLAN, 2000). The storm-wave climate dur-

Table 1. *Amplitude, permanence, and probability of occurrence of astronomic, climatic and tectonic processes affecting relative sea-level changes along the Pacific Northwest coastline.*

Process raising relative sea level (RSL)	Max. Height of RSL rise (m)[a]	Permanence of RSL change[b]	Recurrence interval (yrs)[c]	Source of data
Astronomical tides				
Mean Higher High Water	1.0–1.2	<hour	<1	NOS, 1992
Extreme predicted tides	1.8–2.0	<hour	1–100	SHIH and KOMAR, 1994
Climatic processes				
Seasonal variations	0.2	6 months	1	HUYER *et al.*, 1983
El Niño	0.2–0.4	8 months	4–8	DIAZ and MARKGRAF, 1992; HUYER *et al.*, 1983; KOMAR, 1998
Storm surge	0.2 [0.7–1.6][d]	hours–days	<10	RUGGIERO *et al.*, 1996; MCKINNEY, 1976 [KOMAR *et al.*, in press; PETERSON and DARIENZO, 1996]
Storm-wave runup	2.8–3.3 [3.5–3.9]	seconds–minutes	50–100 [1–100]	TILLOTSON and KOMAR, 1997; [RUGGIERO *et al.*, 1996]
Extreme ocean level (EOL)[e]	1.8–2.5	hours–days	1–100	SHIH and KOMAR, 1994
EOL plus storm-wave runup	4.5–5.2 [5.9–7.6][d]	hours–days	1–10 [100]	RUGGIERO *et al.*, 1996 [KOMAR *et al.*, in press]
Tectonic processes				
Coseismic subsidence	2.5	50–170 years[f]	500–540	ATWATER and HEMPHILL-HALEY, 1997
Remote tsunami runup	6.3	6 hours	200–300	NGDC, 1998
Local tsunami runup	3–12	6–12 hours	500–540	ATWATER and HEMPHILL-HALEY, 1997; PRIEST, 1995

[a] The magnitude of relative sea-level (RSL) rise refers to height above National Geodetic Vertical Datum—1929.
[b] After NELSON *et al.*, 1996b.
[c] Recurrence intervals are arbitrarily selected based on ranges and maximum estimates of recurrence from source. Most of the recurrence intervals are limited to less than 100 years because the time series data used to predict the recurrence intervals are of limited duration.
[d] Brackets denote alternative estimates with corresponding references.
[e] Extreme ocean level (EOL) equal to the sum of astronomical tide, storm surge and/or El Niño.
[f] Permanence estimated as 0.1 to 0.3 times the recurrence interval (520 yr).

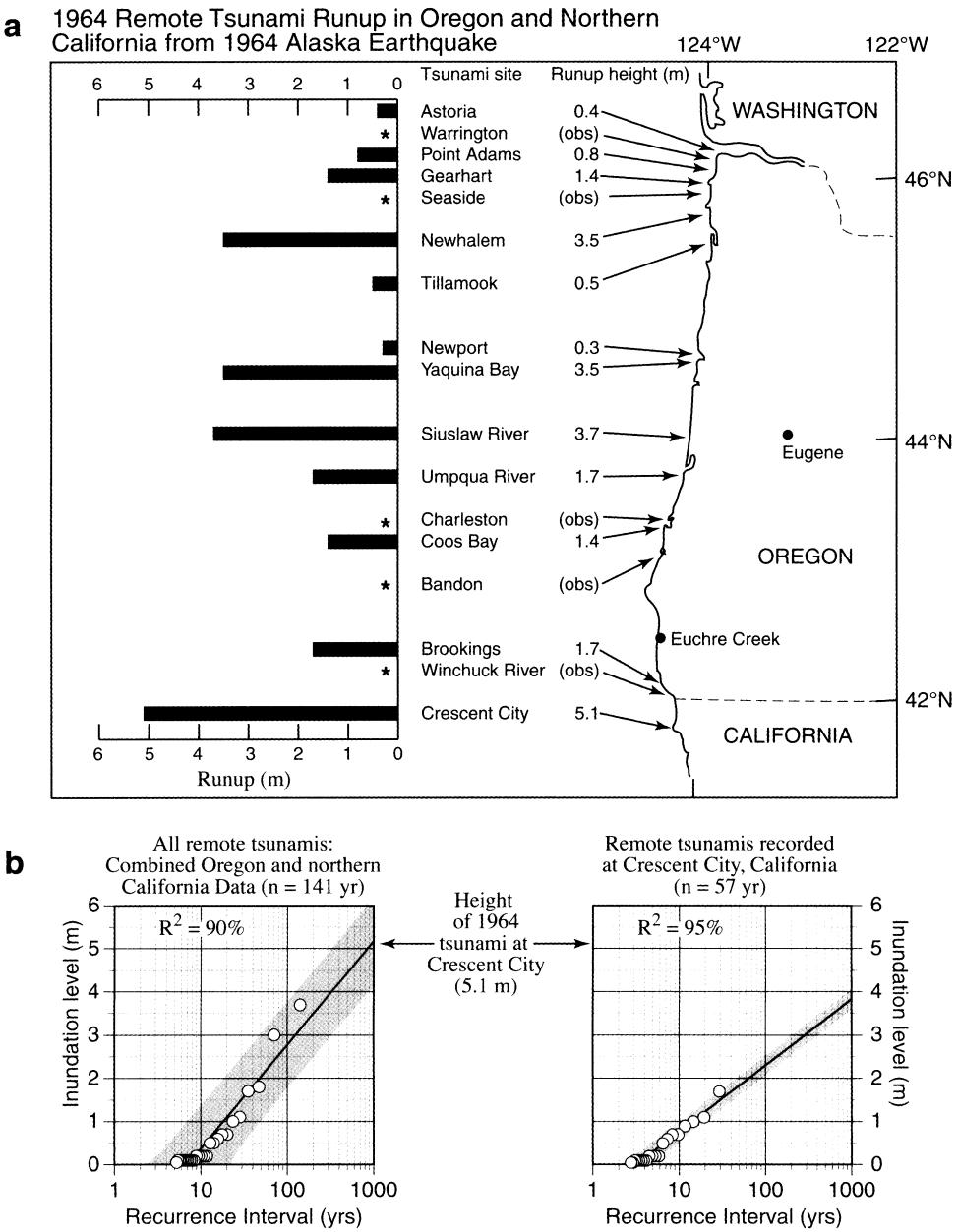

Figure 4. (a) Histogram of the highest remote tsunami runup elevations observed in Oregon bays including Crescent City, California as a result of the 1964 Alaska earthquake. Asterisks and (obs) indicate that waves were observed at the site but runup measurements were unreliable. Runup elevations refer to the height the tsunami reached above a reference level such as mean sea level (NGVD) but it is not always clear which reference level was used (NGDC, 1998). (b) Magnitude-frequency diagrams for all historic remote tsunamis on the Oregon coast including Crescent City, California. Recurrence intervals (RI) for remote tsunamis were determined according to the Weibull equation: RI = (n + 1)/r, where n represents record span in years and r represents the rank of the event in descending order of magnitude. For the left diagram, we used the highest runup documented for each individual remote tsunami, regardless of the location of observation on the Oregon coast including Crescent City. Black arrows mark a 5.1 m runup observed at Crescent City due to a tsunami generated by the 1964 Prince William Sound earthquake in Alaska. The extremely high runup for this tsunami was not used in the linear regression analysis (see text for discussion). Instead, we use a runup of 3.7 m at the Siuslaw estuary, Oregon for the 1964 tsunami. The diagram at right shows the magnitude and recurrence interval relation for all historic remote tsunamis recorded at Crescent City, California. Shaded areas in both diagrams represent the 95% prediction interval for the linear regression line calculated for the tsunami data.

Table 2. *Radiocarbon analyses by accelerator mass spectrometry, Euchre Creek Marsh.*

Core	Depth in core (cm)	Lab number[a]	Dated Material	$^{14}C \pm 1\sigma$ (yr B.P.)	Calibrated age[b]
8	59–63.5	GX21477	Rhizomes	50 ± 50	0–280
6	125–127	GX21476	Seeds, spruce needles	140 ± 50	0–310
6	129	AA19341	Spruce cone, seeds	105 ± 45	0–280
1	137.5–140.5	GX21475	Stems/rhizomes	380 ± 60	0–550
2	140	AA19342	Twigs	195 ± 45	0–420
1	203–214	AA19343	Twigs	1690 ± 65	1360–1820

[a] Radiocarbon laboratory abbreviations: AA, University of Arizona, NSF Accelerator Facility; GX, Geochron Laboratories, Cambridge, Massachusetts.
[b] Calibrated age ranges according to STUIVER and REIMER (1993) calculated with an error multiplier of 1.5 and reported at 2σ.

ing El Niño years may be less severe than non-El Niño years due to the southward displacement of the winter storm track across the coast of south-central California rather than the Pacific Northwest coast (SEYMOUR, 1996). However, storm surges do occur during El Niño years as evidenced by a severe storm in November 1997 at Newport Oregon. During this storm, deep-water significant wave heights reached 10 m, the value previously predicted as the 100-yr storm event (KOMAR *et al.,* in press). The measured tide near the peak of the storm exceeded the predicted tide level by 0.95 m. KOMAR *et al.* (in press) attributed 0.45 m of the measured tide to El Niño processes and 0.4 m to a storm surge that lasted 12 hours.

Storm Surge Magnitudes

A storm surge is the anomalous elevated sea level, augmenting the astronomical tide, that results from wind shear and low atmospheric pressure accompanying a storm. The duration of the surge is related to the duration of storm winds and the amplitude is a function of storm severity and the slope of the continental shelf (PUGH, 1987; ZHANG *et al.,* 1997). The compound effect of storm surge during El Niño years can result in significant differences, on the order of 0.5 m, between predicted and observed extreme tides in Oregon (SHIH *et al.,* 1994). The contribution due to storm surge is poorly studied, although RUGGIERO *et al.* (1996) suggest typical elevations of storm surge on the Oregon coast of 0.13 m based on the standard deviation of a 48 hr low pass filter on the residual time series for a 24 year tidal data set from the Yaquina Bay, Oregon tide gage. MCKINNEY (1976) attributed less than 0.2 m increase in sea level due to storm surge in a survey of specific Oregon storms that caused significant property damage during the spring 1976 erosion of Siletz Spit, Oregon. Although several researchers regard storm surges as a minor component in the equation of extreme ocean levels, PETERSON and DARIENZO (1996) reported a storm surge of 0.5 to 1.2 m on November 13 to 14, 1981 based on measured tide level, atmospheric pressure and wind velocity recorded simultaneously at the Hatfield Marine Science Center at Yaquina Bay, Oregon. Similarly, we found evidence for a 0.5 m storm surge (Figure 3) that occurred during a storm over December 14 to 16, 1997. Differences between measured and predicted tides before and after the December 1997 storm show little influence of increased sea level due to the 1997–98 El Niño indicating that the dominant mechanism forcing the 0.5 m sea-level anomaly in this case was a storm surge.

Additional tidal data that suggest storm surges provide a significant contribution to extreme ocean level on the Pacific Northwest coast come from extreme high water observations at the Toke Point tide gage at Willapa Bay during a non-El Niño winter. Over the course of a three-day storm in early March 1999, the measured tide exceeded the predicted tide by 1.76 m, of which 0.17 m was attributed to seasonal affects on monthly-mean water levels and the remaining 1.6 m was attributed to an intense storm (KOMAR *et al.,* in press). Finally, recurrence interval-magnitude relations for storm surges on the west coast of Vancouver Island computed by HUTCHINSON *et al.* (1997) predict 10 year storm surges with magnitudes >0.5 m and 100 year storm surges with magnitudes of 0.9 to 1.0 m. However, these frequency-magnitude estimates for storm surges neglect to account for the joint sea-level effect contributed by El Niño events (HUTCHINSON, *personal communication*).

Although there are few quantitative analyses of the frequency and magnitude of Oregon storm surges, on the basis of storm surge estimates constructed from tidal data from Yaquina Bay and reports of storm surges elsewhere in the Pacific Northwest, storm surge is an important phenomenon that significantly enhances ocean levels increasing the potential for sand deposition in coastal marshes. To more accurately account for the processes responsible for extreme ocean levels, more detailed quantitative analyses of extreme tide level anomalies within the context of climate patterns are needed.

Storm-Wave Runup

Storm-wave runup on Oregon beaches can reach sufficient magnitudes and provide adequate energy to transport sand into coastal marshes. The highest total water levels, caused by climatic processes, occur as a result of storm-wave runup superimposed upon extreme ocean levels produced by storm surge, El Niño and unusually high astronomical tides. SHIH *et al.* (1994) depict total water levels as a combination of the measured tide, and the vertical component of wave runup. We employ this model to predict the frequency with which extreme ocean levels plus storm-wave runup reach or exceed the elevation of barriers or dunes, resulting potentially in the transport and deposition of sand in the marsh (Figure 2).

RUGGIERO *et al.* (1996) estimate the 2% exceedance elevation for wave runup maxima, $R_{2\%}$, by a linear relationship between wave runup and deep-water significant wave height, H_s,

$$R_{2\%} = 0.5\ H_s - 0.22\ (\text{m})\ (r^2 = 0.72) \quad (1)$$

on low energy dissipative beaches typical of the Oregon coast.

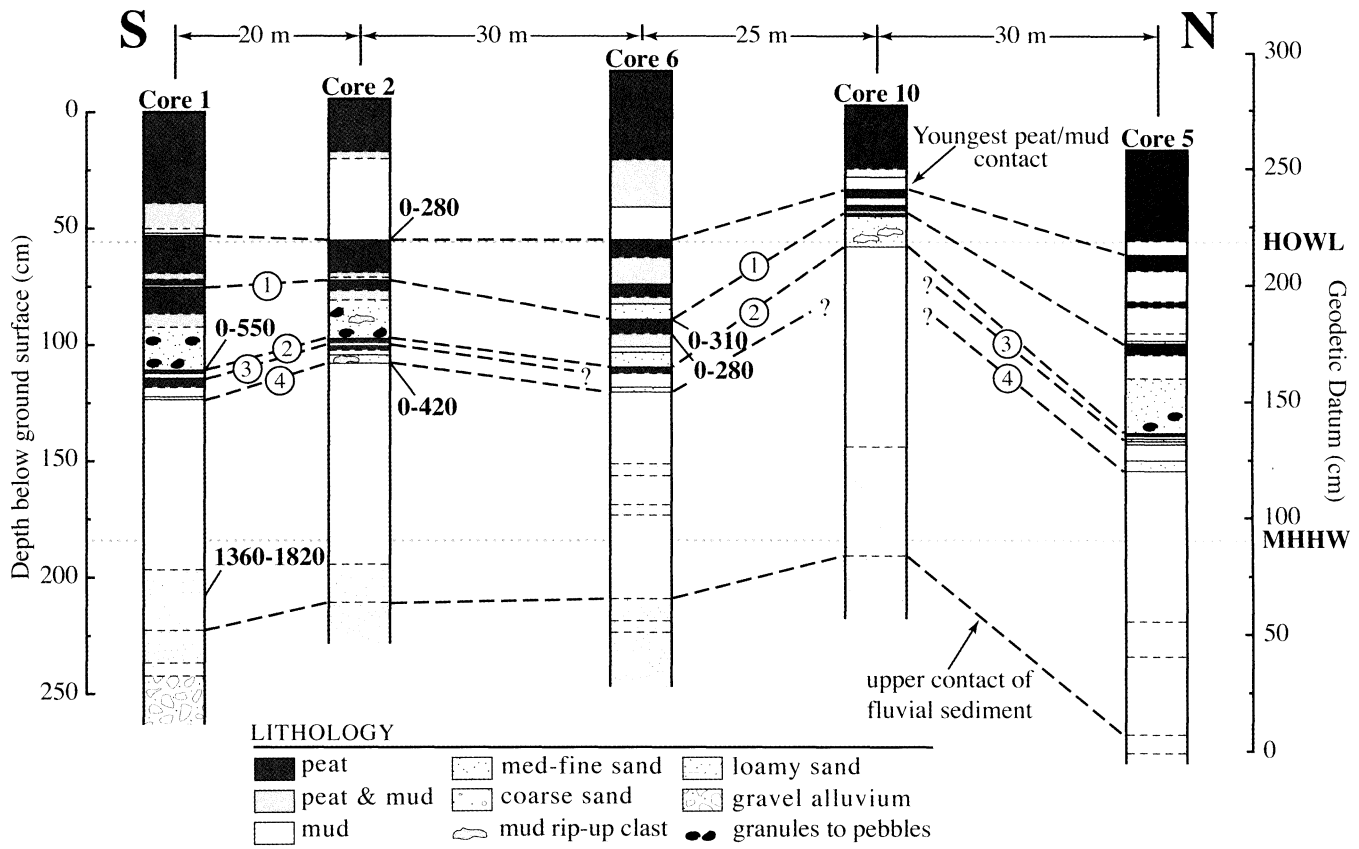

Figure 5. Lithostratigraphy of the sediment underlying the Euchre Creek marsh based on selected 7.5 cm diameter cores. Solid lines separating lithologies denote abrupt (≤3 mm) contacts; dashed lines denote gradual (>3 mm) contacts. Calibrated age ranges are based on radiocarbon analyses of delicate organic material (Table 1). Highest Observed Water Line (HOWL) and Mean Higher High Water (MHHW) referenced to NGVD (NOS, 1992).

Using equation (1), RUGGIERO *et al.* (1996) computed extreme-value probability distributions and recurrence intervals for wave runup based on significant wave height data recorded by offshore buoys. However, more useful for this study are RUGGIERO *et al.*'s (1996) magnitude-frequency analyses for total ocean levels calculated from a joint time series that combines wave height data with extreme measured tide records. Based on these analyses it is plausible for storm waves during extreme water levels on the Oregon coast to exceed 5 m once every 10 years. Extreme ocean levels >5 m could inundate low lying (3 to 5 m) coastal marshes in washover settings such as Euchre Creek.

On the basis of recent tidal and offshore buoy data collected during the 1997–98 El Niño and the winter of 1998–99 it is likely that 5 m underestimates the 10-yr recurrence interval for maximum total water levels on the Oregon coast. KOMAR and ALLAN (2000) observed that one storm during the 1997–98 El Niño generated significant wave heights in excess of 10 m and four storms exceeded that height in the winter of 1998–99 with an additional storm that generated 14 m significant wave heights. The significant wave heights generated by these storms greatly exceeded the 8.2 to 9.1 m values projected as the 100-yr significant wave height by earlier wave climate studies by TILLOTSON and KOMAR (1997) and RUGGIERO *et al.* (1996), respectively. As a result of this new data, KOMAR and ALLAN (2000) increased the predicted 100-yr maximum significant wave height to 16 m. Although estimates of total water levels predicted by joint probability analyses that combine the most recent significant wave height data with extreme measured tide records are not available at this time, KOMAR *et al.* (in press) presented a semi-quantitative analysis of total water levels due to extreme ocean levels and storm wave runup in three scenarios. The first scenario consisted of a 100-yr storm during a non-El Niño winter; the second scenario considered a lesser storm during an El Niño winter; and finally, a third scenario presented the worst case possibility when a 100-yr storm occurs during an El Niño winter. Total water levels predicted by this analysis ranged from 5.87 to 7.63 m (KOMAR *et al.*, in press), sufficiently high to overtop sand barriers and deposit sand in washover environments.

Runup from Remote Tsunami

Subduction zone earthquakes generated at Pacific Rim convergent margins other than the Cascadia subduction zone may generate tsunamis large enough to propagate across the Pacific ocean and deposit sand in Oregon coastal environments. For example, two tsunamis, the first generated by the southern

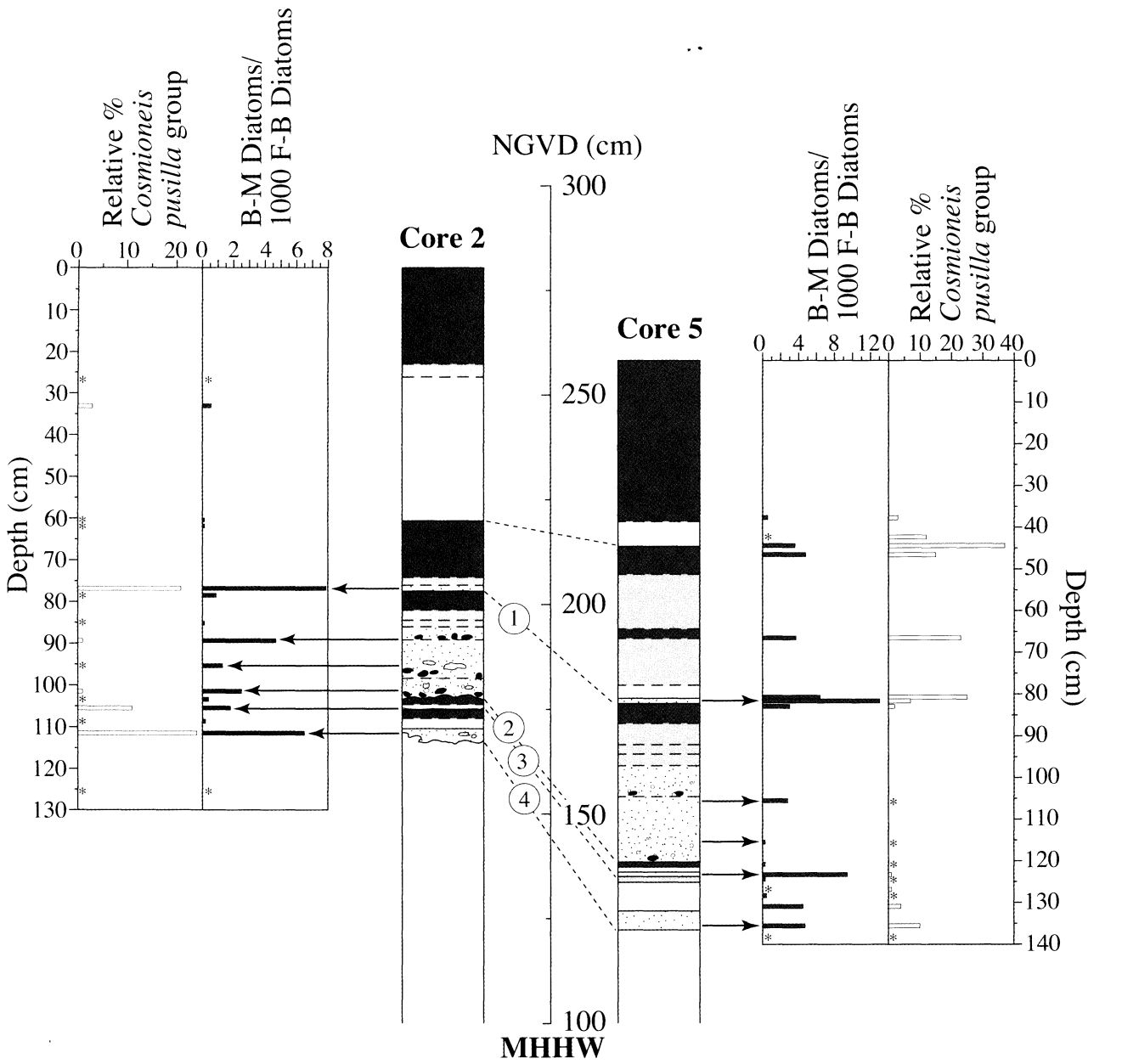

Figure 6. Biostratigraphy depicting five abrupt transitions in lithology in the upper ~1.4 m of sediment in core 2 and core 5 from the Euchre Creek marsh (locations shown in Figure 1). Refer to Figure 5 for explanation of lithology and symbols. Horizontal gray bars represent estimated brackish-marine (B-M) diatoms per 1000 fresh-brackish (F-B) diatoms observed in ~1-cm-thick sediment samples taken from selected lithological horizons. White bars indicate the percent of *Cosmioneis pusilla* group diatoms (indicative of slightly more saline conditions, possibly nearer to a tidal channel) observed relative to the total F-B species observed. Black arrows correspond to diatom samples from the respective sand beds numbered 1 through 4. Asterisks indicate an absence of B-M or *Cosmioneis pusilla* group species.

Chile earthquake of 1960 and the second caused by the 1964 Prince William Sound, Alaska earthquake deposited sand in coastal marshes in northern California and Vancouver Island, British Columbia, Canada (BENSON *et al.*, 1997; CARVER *et al.*, 1996; CLAGUE and BOBROWSKY, 1994b). Because these waves arose from seismicity at subduction zones remote from the Pacific Northwest and traversed the Pacific Ocean to reach the Pacific Northwest, we refer to these potentially devastating waves as remote tsunamis.

The National Geophysical Data Center's Worldwide Tsunami Database (NGDC, 1998) documents 27 remote tsunamis that were observed on the Oregon coast and Crescent City, California since 1854. The highest reported tsunami runup in Oregon, 3.7 m, occurred at the Siuslaw River on 28 March 1964 as a result

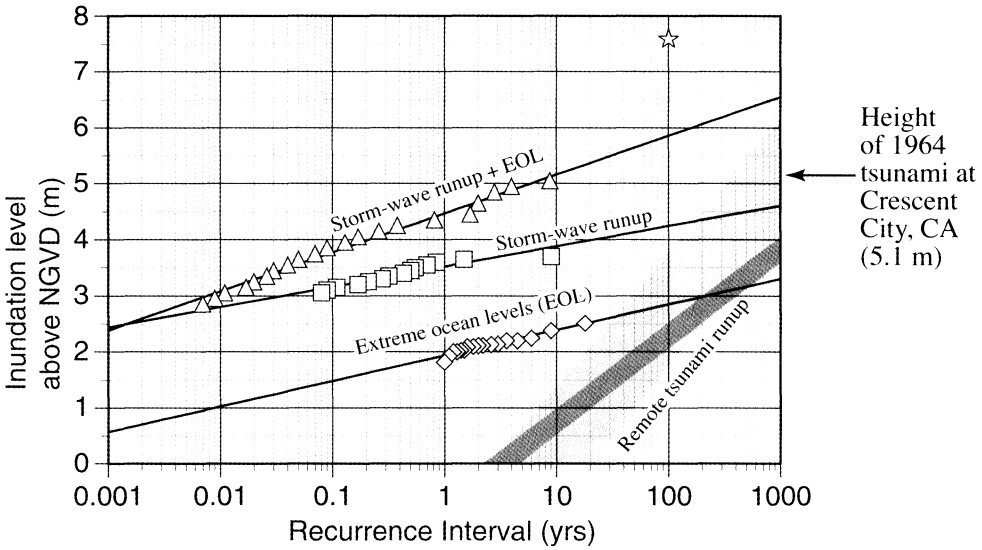

Figure 7. Inundation heights and recurrence intervals for climatic and oceanic processes and remote tsunamis. Open triangles and boxes represent extreme-value probability distribution and recurrence intervals for total water levels (wave runup plus extreme ocean levels, EOL) and storm-wave runup, respectively, calculated from time series of extreme wave height and measured tide data from the Yaquina Bay tide gage (RUGGIERO *et al.*, 1996). Open diamond symbols mark extreme ocean level (EOL, highest annual measured tides) recorded at the Yaquina Bay tide gage between 1967 to 1974 and 1982 to 1997, representative of the combined sea-level enhancement due to storm surges, El Niño conditions, seasonal effect on ocean level, and/or high astronomical tides. The shaded regions represent the 95% prediction interval for the linear regression line calculated for both tsunami data sets shown in Figure 4b. The star indicates the maximum total water level for a 100-yr storm predicted from analyses of deep-water significant wave height data recorded during extreme storms during the 1997–98 El Niño and the winter of 1998–99 (KOMAR *et al.*, in press).

of the Prince William Sound earthquake in Alaska (Figure 4a). The 1964 Alaska tsunami reached unusually high runup elevations compared to other remote tsunamis in the data base because the arrival of the wave coincided with a high spring tide (WILSON and TØRUM, 1968). For instance, the 5.1 m maximum tsunami runup that devastated Crescent City in 1964 plotted as an outlier in a log-normal frequency-magnitude relationship of all remote tsunamis recorded at Crescent City (Figure 4b). One explanation for the exceptional runup height for this tsunami, in addition to the joint occurrence of a high spring tide, may be that the nearshore bathymetry offshore Crescent City may act to focus wave energy leading to higher wave runup than at other coastal sites. Because of this anomalous runup elevation, we did not include the 1964 remote tsunami at Crescent City in the linear regressions shown in the magnitude-frequency diagrams (Figure 4b). Based on these analyses, remote tsunamis attacking the Oregon coast with runup elevations of 5 m may have recurrence intervals of several hundred years. Because the recurrence interval of remote tsunamis with runup of 5 m is far greater than the recurrence of Pacific storms with wave runup of 5 m, we infer that there is a possibility of recording remote tsunamis in marsh stratigraphic records, but that the probability of depositing sand by remote tsunami is less than the probability of depositing sand by wave runup during storm and extreme ocean levels combined.

Coseismic Subsidence

Abrupt subsidence during a plate-interface earthquake can create more favorable conditions for sand deposition in coastal marshes. Coseismic subsidence of 0.3 to 0.8 m, based on a simple model of relative sea-level response to the seismic cycle, results in tide levels closer to the elevation of supratidal marshes and washover settings. The resulting abrupt rise in relative sea level may bring marsh environments, formerly out of reach of extreme ocean levels and remote tsunamis, into closer proximity of the maximum inundation levels for sand depositional mechanisms. Table 1 shows an estimate of the duration that an environment will be susceptible to inundation by marine waters based on a simple model of the seismic cycle that involves coseismic subsidence followed by interseismic uplift (ATWATER and HEMPHILL-HALEY, 1997). We assume that post-seismic and interseismic rebound following an earthquake cause relative sea-level fall such that within 50 to 170 years the marsh environment is restored to the same relative elevation that it had prior to the earthquake. Thus, coseismic subsidence would temporarily decrease the critical elevation necessary for marine inundation of coastal marshes and lakes.

Local Tsunamis

Heights attained by local tsunamis generated by great earthquakes on the Cascadia subduction zone have been estimated from numerical models. Modeling predicts wave heights between 3 to 12 m striking the outer Oregon coast within 14 to 30 minutes of an earthquake of M_w = 8.8 to 8.9 (PRIEST, 1995). Maximum runup elevations for tsunamis of any origin may be highly variable for specific coastal locations because of complex effects on wave propagation owing to the geometry of sea-floor deformation, nearshore bathymetry and coastal refraction.

Thus, numerical simulations provide only an approximation of maximum runup elevations. An independent record of late Holocene tsunami and extreme storm-wave runup magnitude and frequency may be obtained from the stratigraphic records beneath coastal marshes within the vertical inundation zone for these phenomena. We use an earthquake recurrence interval of 500 to 540 years, estimated for the Cascadia subduction zone by ATWATER and HEMPHILL-HALEY (1997), as a proxy for the frequency of local tsunamis. We investigated the Euchre Creek marsh for stratigraphic evidence of local tsunamis and to assess whether sand beds deposited by storm events or remote tsunamis were also preserved in the sedimentary record.

STUDY SITE AND METHODS

The Euchre Creek marsh (Figure 1) is vulnerable to sand deposition by local tsunamis generated by seafloor dislocation during earthquakes on the Cascadia subduction zone, remote tsunamis generated elsewhere in the Pacific Rim, and extreme ocean levels brought about by a combination of high astronomical tides, El Niño and storm conditions. To assess the relative importance of tsunamis and storm-wave runup during extreme ocean levels as sand-depositional processes, we investigated the lithology, diatom paleoecology and chronology of 4 anomalous sand beds in the stratigraphic sections beneath the 2.5 ha Euchre Creek marsh, 33 km south of Cape Blanco, Oregon (Figure 1c). The marsh occupies an abandoned river channel incised into late Pleistocene fluvial deposits about 0.5 km east of the Pacific Ocean and is protected from the open ocean by a barrier of dune sand 6 to 8 m high. However, the ocean has access to the marsh via the mouth of Euchre Creek where the coastal deflation plain and floodbanks do not exceed 3 m in elevation.

Ten 7.5-cm-diameter cores were obtained by driving plastic drainage pipe into the marsh with a sledge hammer. The pipe was removed with a winch mounted on a step ladder. We recommend using core catchers for consistent recovery of sediment. Exploratory 2.5-cm-diameter gouge cores located between the sites of the larger cores were used to correct for compaction and confirmed the continuity of stratigraphic beds.

We cleaned diatom samples with 30% H_2O_2. An aliquot of this solution was transferred to a 22 × 30 mm cover slip and affixed to a glass slide with Naphrax mounting medium. Numbers of brackish-marine species were tallied in 20 vertical traverses of the slide. We estimated the numbers of fresh-brackish diatoms in 20 traverses from the average counted in 5 traverses (Appendix A).

Radiocarbon samples were selected from sand beds or peaty soils directly underlying sand deposits (Table 2). Samples consisted of delicate plant fossils, unlikely to survive extensive transport and redeposition, such as spruce needles and cones, seeds and twigs with intact bark; thus, the ages approximate the time when the material was deposited. Accelerator mass spectrometry radiocarbon ages were calibrated according to STUIVER and REIMER (1993).

BIOSTRATIGRAPHY AND SEDIMENTOLOGY

We mapped the subsurface stratigraphy in the southeast portion of the marsh through a series of core transects trending N 32° E (Figure 1c). Coring was restricted to this area because exploratory probes in the western portion of the marsh encountered impenetrable sandy sediment owing to the proximity of nearby dunes and the beach. All cores record marsh inception prior to 1400 yr B.P. as the gradual transition upward from alluvial gravel to sandy loam sediment (Figure 5). Diatom analyses indicate a fresh-brackish marsh during this transition with intermittent standing water.

Unlike the poorly sorted fluvial gravel and lithic rich sand at the base of the section, the overlying four sand beds (events 1–4, Figure 5) consist of medium-fine, sub-rounded, well sorted grains and are similar in texture and mineralogy to neighboring beach and dune sand. Because brackish-marine diatoms occur within each of these four sand beds, we infer a marine source for the sand. Events 1 and 2 correlate across the entire marsh (Figure 5), but events 3 and 4 are discontinuous and unrecognized in the central portion of the core transect (*e.g.,* core 10, Figure 5). The uppermost peat-mud contact records a flood of Euchre Creek in December of 1955 (HOFMANN and RANTZ, 1963) that deposited ≥12 cm of mud over the marsh. The four sand deposits are discussed in order from those that are thinner and less widely distributed to those that are thickest and laterally most extensive.

The discontinuous deposits of events 3 and 4 consist of clean, fine sand abruptly overlying mud or an incipient peaty soil (Figure 5). The sand layer of event 4 incorporates mud clasts above an irregular lower contact indicating erosive emplacement. Brackish-marine diatoms are present in both sand beds and include the species *Thalassiosira pacifica,* which is prominent in littoral plankton and swash-zone beach deposits on the modern coast (Figure 6).

The thick (5 to 22 cm), laterally continuous sand sheet of event 2 abruptly buries a 1-to-2-cm-thick peat horizon and consists of 2 to 3 fining upward intervals of medium-to-fine sand with pebbles at the base of each interval (Figure 5). On the basis of the pebbles and mud-rip-up clasts incorporated within the sand, as well as the fining upward intervals, we infer that repeated high energy currents deposited the sand during several cycles of inundation. Further, sparse brackish-marine diatoms preserved within the sand layer indicate a marine origin (Figure 6).

The event 1 sand consists of a 1-to-2-cm-thick, well sorted medium-to-fine continuous sand sheet (Figure 5). The sand fines upward and in some cases incorporates small pebbles near its base. This sand abruptly overlies a peat horizon and is overlain, in turn, by mud or peaty mud that grades upward into the uppermost buried marsh soil. In core 5, the mud overlying the sand was 11.5 cm thick. Brackish marine diatoms are present in the event 1 sand layer in both cores 2 and 5 (Figure 6). Relative to core 2, diatoms in core 5 are better preserved and include a diverse group of species commonly found on tidal flats and in sloughs. Diatoms in marsh deposits above the event 1 sand layer in core 5 show an increase in salinity-tolerant species, particularly the high salt marsh diatom group *Cosmioneis pusilla* (ATWATER and HEMPHILL-HALEY, 1997). Although the sand sheet in core 2 contains similar fresh-brackish species, they were not as well preserved suggesting higher salinities at the northern core site (core 5), which is about 0.5 m lower and closer to the potential path of extreme ocean waters to the northwest (Figure 6).

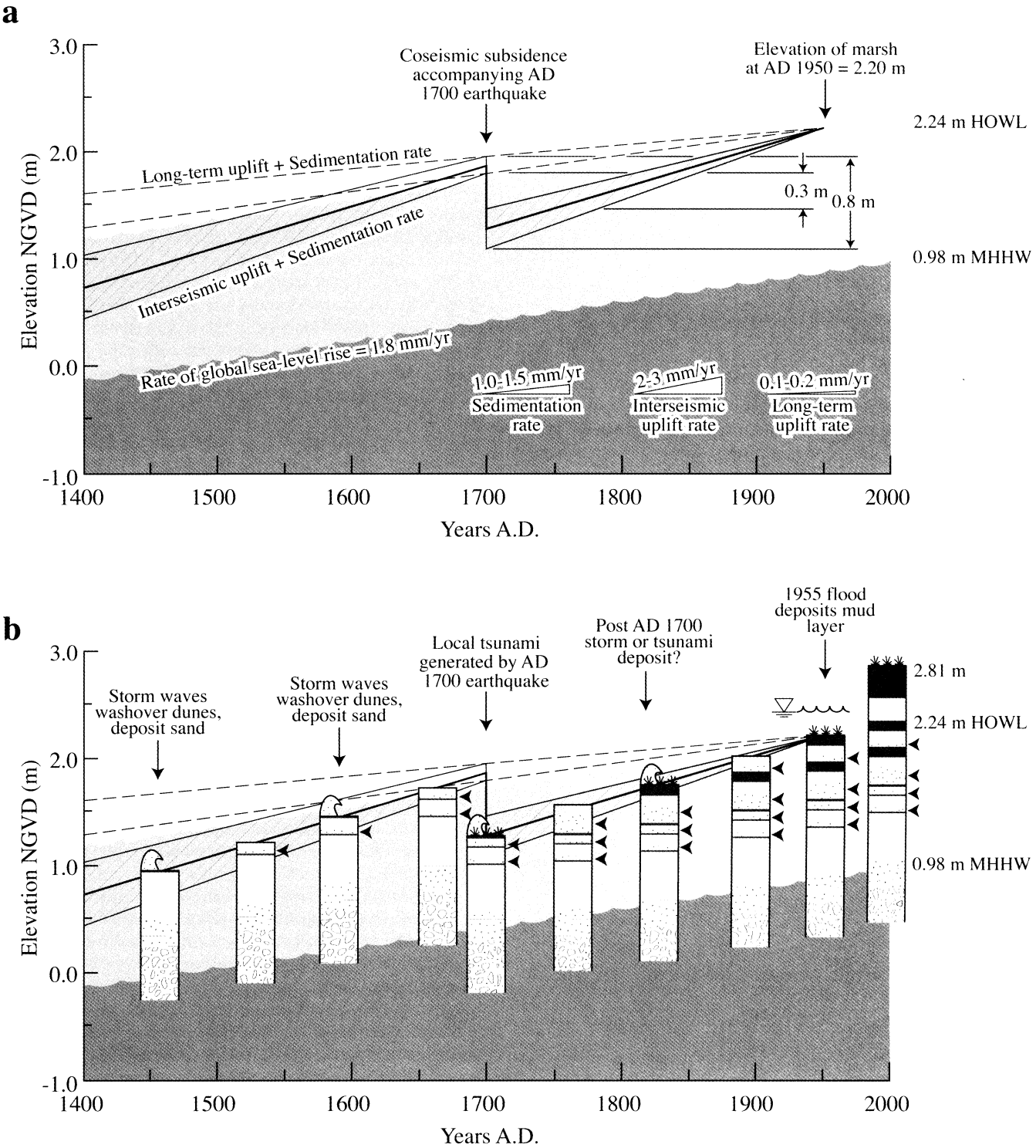

Figure 8. (a) Simple graphical model of the effect of the seismic cycle on marsh surface elevation over 600 years of sedimentation at Euchre Creek. Dashed lines bracket the minimum and maximum constraints on the sum of long-term uplift rate and marsh sedimentation rate (1–1.5 mm/yr). Bold black line depicts emergence of marsh surface over time as a result of combined interseismic uplift and marsh sedimentation rates (3 to 4.5 mm/yr), interrupted by sudden coseismic subsidence during the A.D. 1700 Cascadia earthquake. Area filled with diagonal lines represents maximum and minimum constraints on marsh emergence. Post-seismic marsh elevation at A.D. 1700 ranged between 1.2 to 1.6 m based on surface elevation extrapolated from present-day uplift rate and the marsh sedimentation rate. Using long-term uplift rates plus sedimentation rates as an upper constraint on the preseismic elevation of the marsh, this model predicts between 0.3 to 0.8 m of subsidence at Euchre Creek as a result of the A.D. 1700 earthquake. HOWL, highest observed water level; MHHW, mean higher high water based on Port Orford tide gage (NOS, 1988). Light grey (HOWL), and dark grey (MHHW) areas

In summary, while all four sand deposits are well sorted and medium-to-fine in texture, display abrupt lower contacts and have brackish marine diatoms from which we infer their source was from the ocean, they differ in other physical attributes. Only event 2 and 4 deposits have evidence for erosion at the basal contacts. Only event 1 and 2 sands are a continuous sheet-like deposit throughout the wetland and only event 2 sand has multiple fining-upward pulses. None of the sand deposits have strong biostratigraphic evidence for subsidence accompanying deposition, although one interpretation of the diatom paleoecologic changes accompanying deposition of event 1 sand is that the site subsided at the time of sand deposition. From these observations, we infer that all of the sand deposits were emplaced by high-energy marine waters, which limits the emplacement mechanism to extreme ocean levels and wave runup during a storm or tsunami.

DISCUSSION

Reconstructing Stratigraphic Records of Inundation by Tsunamis and Storm Waves

Several problems complicate efforts to recognize or distinguish the candidate processes that deposited sand beds preserved in stratigraphic records. For example, sand beds deposited by wave runup during storm surges have the same marine provenance as both local and remote tsunamis. Furthermore, despite some investigations that conclude historic storm surge deposits display unique sedimentary structures (MEI-E *et al.,* 1985; NISHIMURA and MIYAJI, 1996), most researchers conclude that sand beds preserved in geologic records do not display unique physical characteristics that would unequivocally distinguish between storms or tsunamis as the depositional mechanism (FOSTER *et al.,* 1991; SATO *et al.,* 1995).

An alternative method to infer the depositional mechanism of sand beds preserved in marsh sediments is to identify the candidate mechanisms that could deposit sand in similar coastal settings, analyze the magnitude and recurrence intervals of these processes and then compare the results to the frequency of sand beds in the geologic record. Following this method, we first compared the recurrence interval of local tsunamis generated by great earthquakes on the Cascadia subduction zone (RI = 500 to 540 yr) to the recurrence interval of events that deposited sand in the Euchre Creek marsh (4 sand beds deposited within the last 600 years; RI = 150 yr). Because the recurrence interval of sand deposition at Euchre Creek is smaller than the recurrence interval estimated for local tsunamis, other marine processes must have transported and deposited sand in the Euchre Creek marsh. Frequency-magnitude analyses of climatic events and remote tsunamis (Figure 7) suggest that the most likely alternative mechanism for depositing sand in settings similar to Euchre Creek is storm wave washover during periods of extreme ocean level. Although historic records report that the 1964 remote tsunami that devastated Crescent City attained a runup elevation of 5.1 meters (Figure 4), magnitude-frequency analyses show that remote tsunamis of this severity have recurrence intervals of several hundred years and are similar in magnitude to storm-wave runup during extreme ocean levels with recurrence intervals of 10 years (Figure 7).

Marsh sedimentation rates, vertical deformation as a result of the seismic cycle, and global sea-level rise all must be considered to determine the relative elevation of the marsh with respect to sea level over the past 600 years. By determining the change in elevation of the marsh during the past 600 years, we can deduce whether alternative mechanisms for sand deposition were more or less likely to cause inundation of the marsh. Figure 8 shows a simple model of marsh emergence and abrupt subsidence in response to the seismic cycle assuming constant rates of long-term tectonic uplift of Pleistocene wave-cut platforms (KELSEY and BOCKHEIM, 1994), interseismic uplift from tide gage and geodetic leveling data (MITCHELL *et al.,* 1994) and marsh sedimentation that can be used to reconstruct former marsh surface elevations. KELSEY *et al.* (1998) used a similar model to estimate the magnitude of coseismic subsidence and relative sea-level rise due to the A.D. 1700 Cascadia earthquake at the Sixes River, ~30 km north of Euchre Creek. Using these constraints on relative sea level, we conclude that the surface was within 0.6 to 0.9 m above mean higher high water (compared to the present difference of 1.8 m) following inferred coseismic subsidence during the A.D. 1700 earthquake. Furthermore, the elevation of mean higher high water was closer to the marsh surface elevation at all times in the past except for a period of about 100 years prior to the A.D. 1700 earthquake. Thus, if the elevation of the marsh was influenced by the seismic cycle, there would have been a higher probability that storm-wave washover during extreme ocean levels would have inundated the marsh in the past because the elevation of the marsh was lower with respect to sea level.

Record of Storm-Wave Washover and Tsunamis at Euchre Creek, Oregon

Well preserved brackish-marine diatoms in each of the sand beds suggest rapid deposition from a marine source indicating one of three possible depositional mechanisms: (1) storm-wave runup superimposed on extreme ocean levels; (2) remote tsunami, or; (3) local tsunami generated by an earthquake on the Cascadia subduction zone. Considering an average earthquake recurrence interval of 500 to 540 years for the Cascadia subduction zone (ATWATER and HEMPHILL-HALEY, 1997), a 150 year recurrence interval for sand sheets in the marsh at Euchre

←

represents sea-level datum projected back in time based on 1.8 mm/yr rate of global sea-level rise (DOUGLAS, 1991). Long-term uplift rates, 0.1 to 0.2 mm/yr, estimated from studies of Pleistocene marine terraces in southern Oregon (KELSEY and BOCKHEIM, 1994). Interseismic (present-day) uplift rates, 2 to 3 mm/yr, derived from tide gage and geodetic leveling data investigated by MITCHELL *et al.* (1994) (b) Schematic depiction of marsh stratigraphic development since 550 yr B.P. Horizontal arrowheads mark position at hypothetical time of deposition of sand layers 1–4. Based on this model of marsh development in response to the seismic cycle, the elevation of the Euchre Creek marsh was closer to MHHW than today at all times in the 600 year history of sedimentation except for a short interval prior to the A.D. 1700 earthquake. As a result, storm-wave runup superimposed on extreme ocean levels (represented by the proxy datum HOWL) was more likely to inundate the marsh in the past.

Creek is too low to attribute to local tsunamis generated by prehistoric great earthquakes on the Cascadia subduction zone. Because the frequency of sand deposits is higher than that expected due to local tsunamis, and based on frequency-magnitude analyses that show storm-wave runup as the most plausible alternative depositional mechanism (Figure 7), we conclude that at least two of the four sand deposits are the result of extreme storm conditions that resulted in wave washover in the marsh and left behind localized deposits of intertidal sand.

The sand sheet of event 2 is the best candidate for a tsunami deposit accompanying the A.D. 1700 earthquake because it displays pulsed deposition, has diatom evidence for a marine source and displays physical attributes of high energy emplacement (Figure 4). Furthermore, tsunami deposits attributed to the A.D. 1700 earthquake are documented to the north and south of Euchre Creek (ATWATER *et al.,* 1995). However, neither fossil diatoms present in the peaty mud overlying the sand, nor the peaty-mud lithology indicate >0.5 m of submergence of the marsh following sand deposition. Evidence for submergence can strengthen the argument for tsunami deposition because widespread buried soils are commonly cited as evidence for coseismic subsidence during subduction earthquakes (ATWATER *et al.,* 1995; NELSON *et al.,* 1996b). A simple model of the response of marsh elevation to the seismic cycle (Figure 8) predicts 0.3 to 0.8 m of subsidence accompanying the A.D. 1700 earthquake. If subsidence did occur, then it was insufficient in magnitude to submerge Euchre Creek below mean higher high water, otherwise diatom analyses would have indicated a paleoecological change from a fresh/brackish marsh to a salt marsh environment.

The sparse abundance and poor preservation of brackish-marine and fresh-brackish diatoms in the event 2 sand may be a function of source material being the nearby dunes to the west, which contain sparse reworked diatoms when compared to abundant diatom populations found in intertidal deposits. Based on this evidence, the wave depositing the event 2 sand may have overtopped and mobilized the dunes (3 to 8 m elevation) west of the marsh. Therefore, of all the sand deposits in the profile, the process responsible for the deposition of the event 2 sand sheet is most consistent with a local tsunami.

We interpret the sand sheet of event 1 as a potential tsunami deposit post-dating the A.D. 1700 earthquake. However, due to equivocal evidence for >0.5 m of coseismic subsidence, we retain storm surge and remote tsunami as a viable interpretation for the depositional process. Not all of the units overlying the sand sheet contain significant quantities of fine grained inorganic sediment which would result from an abrupt rise in relative sea level in response to widespread coseismic subsidence (NELSON *et al.,* 1996a; SHENNAN *et al.,* 1998). Whereas the event 1 sand does not have multiple fining upward cycles, it is laterally continuous and exhibits equivocal paleoecologic evidence that it was accompanied by ≥0.5 m of subsidence, which if the case, would indicate that the sand was deposited during a Cascadia earthquake that coseismically lowered the coastline.

If the event 1 sand records tsunami deposition, then it may indicate that two Cascadia subduction zone earthquakes occurred in the last 600 years. This interpretation is problematic because there is only one well documented earthquake within the last 600 years in Cascadia for sites north of Euchre Creek (ATWATER and HEMPHILL-HALEY, 1997). If Euchre Creek does record two local tsunamis within the last 600 years, then one of the subduction zone earthquakes must have been limited to the southern portion of the Cascadia margin.

We cannot unequivocally differentiate storm generated sand beds from tsunami deposits in stratigraphic records on the basis of their biostratigraphic and physical characteristics. However, because the number of sand beds preserved beneath the Euchre Creek marsh are more than what would be expected based on a local tsunami recurrence interval of 500 to 540 years, other episodes of marine inundation of the marsh, other than local tsunami, must have occurred. Based on frequency-magnitude comparisons of extreme ocean levels augmented by storm-wave runup and historic remote tsunamis observed on the Oregon coast (Figure 7), we infer that the additional sand beds preserved beneath the Euchre Creek marsh (Events 3 and 4; Figure 5) record wave washover during Pacific storms.

SUMMARY AND CONCLUSIONS

Low-lying coastal washover settings, within 3 to 5 m of mean sea level, are susceptible to sand deposition by climatically and tectonically driven marine waves. The washover settings on the Oregon coast considered in this paper include marshes, lakes and lagoons. Because these environments are frequently freshwater habitats, stratigraphic evidence for coincident coseismic subsidence during sand emplacement may be absent. As a result, it may be difficult or impossible to identify the principle depositional mechanism for sand beds in stratigraphic sequences by relying on biostratigraphic and physical characteristics alone. We present a case study that investigates stratigraphic sequences, preserved beneath the freshwater Euchre Creek marsh, which harbor evidence for four episodes of marine sand deposition over the past 600 years—too many to be explained solely by local tsunamis that have inferred recurrence intervals of 500 to 540 years. On the basis of magnitude frequency analyses for alternative depositional mechanisms likely to deposit sand beds in washover settings including storm-wave runup during extreme ocean levels and remote tsunamis generated by subduction earthquakes elsewhere in the Pacific Rim, we arrive at the following conclusions:

(1) Sand beds in coastal stratigraphic sequences do not exhibit physical or textural characteristics that allow the distinction between tsunamis versus storm waves as mechanisms of deposition.

(2) Magnitude-frequency analyses of alternative sand depositional mechanisms other than local tsunami, including storm-wave runup during extreme ocean levels and remote tsunamis, show that these processes can attain inundation height >5 m at recurrence intervals from 10 to 100 years. Thus, sand beds preserved in Oregon marshes, lagoons and lakes may record remote tsunamis or storm-related inundation in addition to local tsunamis. If these alternative processes are not considered, the frequency of local tsunamis as recognized in the geologic record may be overestimated.

(3) Assuming an earthquake recurrence interval of 500 to 540 years (ATWATER and HEMPHILL-HALEY, 1997), at most only two of the four sand sheets preserved beneath the Euchre Creek marsh within the last 600 years are likely to have been depos-

ited by local tsunamis. We conclude that sand sheet 2 was deposited by a local tsunami that accompanied the A.D. 1700 Cascadia earthquake because it is the thickest sand layer in the section, shows evidence of repeated wave inundation, and contains sparse, poorly preserved brackish-marine diatoms reflecting a dune source for the sand. On the basis of this evidence, we infer that the wave that deposited sand 2 overtopped and mobilized dunes with maximum heights of <8 m.

(4) Storm-wave runup during extreme ocean levels that exceed runup heights of 5 m have recurrence intervals equal to 10 years based on extreme value-probability distribution and recurrence interval analyses by RUGGIERO *et al.* (1996). Recent analyses of significant wave height data from the 1997–98 El Niño and the winter of 1998–99 suggest total water levels may exceed 7 m every century (KOMAR *et al.,* in press). In contrast, recurrence intervals of several hundred years are predicted from a Weibull distribution for historic remote tsunamis of equal magnitude on the Oregon coast. Although, we cannot rule out remote tsunamis, storm-wave runup represents a more probable alternative to local tsunami, as the most plausible depositional mechanism for the remaining anomalous sand beds preserved in stratigraphic sequences beneath Euchre Creek.

(5) A simple model of relative sea-level response to the seismic cycle predicts that the marsh was more susceptible in the past to marine inundation by climatic and tectonic processes that generate extreme wave runup >5 m. Global sea-level rise, coseismic and interseismic deformation and sedimentation at the Euchre Creek marsh together produced higher relative sea level elevations with respect to the marsh surface than present over much of the past 600 years. The only time the marsh surface elevation may have been higher with respect to sea level was during the 100 years preceding the last great Cascadia earthquake that occurred in A.D. 1700.

(6) Quantitative analyses of extreme ocean levels, determined from measured versus predicted tide level differences, must investigate frequency variations on time scales similar in duration to Pacific storms to better understand the magnitude and recurrence intervals of storm surges in the Pacific Northwest.

(7) Sediment budgets for Oregon marshes are poorly understood. New investigations that focus on the sedimentologic impact of extreme climatic events like El Niño and severe Pacific storms on rates of sedimentation will contribute useful data for future stratigraphic investigations of sediment response to the seismic cycle in coastal marshes of Oregon.

ACKNOWLEDGMENTS

Support from the Geological Society of America (5742-95) and the National Science Foundation (EAR-9405263). R. Langridge, J. Pickering, and T. Riordon assisted with marsh coring. A. Nelson provided field equipment and review. W. Moore allowed access to his property. P. Komar provided constructive review.

LITERATURE CITED

ATWATER, B.F. and HEMPHILL-HALEY, E., 1997. *Recurrence intervals for great earthquakes of the past 3500 years at northeastern Willapa Bay, Washington.* U.S. Geological Survey Professional Paper 1576, 108p.

ATWATER, B.F. and MOORE, A.L., 1992. A tsunami about 1000 years ago in Puget Sound, Washington. *Science,* 258, 1614–1617.

ATWATER, B.F.; NELSON, A.R.; CLAGUE, J.J.; CARVER, G.A.; YAMAGUCHI, D.K.; BOBROWSKY, P.Y.; BOURGEOIS, J.; DARIENZO, M.E.; GRANT, W.C.; HEMPHILL-HALEY, E.; KELSEY, H.M.; JACOBY, G.C.; NISHENKO, S.P.; PALMER, S.P.; PETERSON, C.D., and REINHART, M.A., 1995. Summary of coastal geologic evidence for past great earthquakes at the Cascadia Subduction Zone. *Earthquake Spectra,* 11, 1–18.

BENSON, B.E.; GRIMM, K.A., and CLAGUE, J.J., 1997. Tsunami deposits beneath tidal marshes on northwestern Vancouver Island, British Columbia. *Quaternary Research,* 48, 192–204.

CARVER, G.A.; PETERSON, C.D.; GARRISON, C.E., and KOEHLER, R., 1996. Paleotsunami evidence of subduction earthquakes from northern California. *Geological Society of America Abstracts with Programs,* 28, A55.

CLAGUE, J.J. and BOBROWSKY, P.T., 1994a. Evidence for a large earthquake and tsunami 100–400 years ago on western Vancouver Island, British Columbia. *Quaternary Research,* 41, 176–184.

CLAGUE, J.J. and BOBROWSKY, P.T., 1994b. Tsunami deposits beneath tidal marshes on Vancouver Island, British Columbia. *Geological Society of America Bulletin,* 106, 1293–1303.

CLIFTON, H.E., 1969. Beach lamination: Nature and origin. *Marine Geology,* 7, 553–559.

COCH, N.K., 1994. Geological effects of hurricanes. *Geomorphology,* 10, 37–63.

DARIENZO, M.E. and PETERSON, C.D., 1990. Episodic tectonic subsidence of late Holocene salt marshes, Northern Oregon Central Cascadia Margin. *Tectonics,* 9, 1–22.

DARIENZO, M.E.; PETERSON, C.D. and CLOUGH, C., 1994. Stratigraphic evidence for great subduction-zone earthquakes at four estuaries in northern Oregon, U.S.A. *Journal of Coastal Research,* 10, 850–876.

DIAZ, H.F. and MARKGRAF, V., 1992. *El Niño: Historical and Paleoclimatic Aspects of the Southern Oscillation.* Cambridge: Cambridge University Press, pp. 476.

DOUGLAS, B.C., 1991. Global sea level rise. *Journal of Geophysical Research,* 96, 6981–6992.

FOSTER, I.D.L.; ALBON, A.J.; BARDELL, K.M.; FLETCHER, J.L.; JARDINE, T.C.; MOTHERS, R.J.; PRITCHARD, M.A., and TURNER, S.E., 1991. High energy coastal sedimentary deposits; an evaluation of depositional processes in southwest England. *Earth Surface Processes and Landforms,* 16, 341–356.

GOODBRED, S.L., JR. and HINE, A.C., 1995. Coastal storm deposition: Salt-marsh response to a severe extratropical storm, March 1993, west-central Florida. *Geology,* 23, 679–682.

HEMPHILL-HALEY, E., 1995. Diatom evidence for earthquake-induced subsidence and tsunami 300 years ago in southern coastal Washington. *Geological Society of America Bulletin,* 107, 367–378.

HOFMANN, W. and RANTZ, S.E., 1963. *Floods of December 1955–January 1956 in the far western states, Part 1: Description.* U. S. Geological Survey Water Supply Paper 1650-A, 156p.

HUTCHINSON, I.; CLAGUE, J.J., and MATHEWES, R.W., 1997. Reconstructing the tsunami record on an emerging coast: a case study of Kanim Lake, Vancouver Island, British Columbia, Canada. *Journal of Coastal Research,* 13, 545–553.

HUYER, A.; GILBERT, W.E., and PITTOCK, H.L., 1983. Anomalous sea levels at Newport, Oregon, during the 1982–83 El Niño. *Coastal Oceanography and Climatology News,* 5, 37–39.

KELSEY, H.M. and BOCKHEIM, J.G., 1994. Coastal landscape evolution as a function of eustasy and surface uplift rate, Cascadia margin, southern Oregon. *Geological Society of America Bulletin,* 106, 840–854.

KELSEY, H.M.; WITTER, R.C., and HEMPHILL-HALEY, E., 1998. Response of a small Oregon estuary to coseismic subsidence and postseismic uplift in the past 300 years. *Geology,* 26, 231–234.

KOMAR, P.D., 1986. The 1982–1983 El Niño and erosion on the coast of Oregon. *Shore and Beach,* 54, 3–12.

KOMAR, P.D., 1998. The 1997–98 El Niño and erosion on the Oregon coast. *Shore & Beach,* 66, 33–41.

KOMAR, P.D. and ALLAN, J.C., 2000. Analyses of extreme waves and

water levels on the Pacific Northwest coast. Report to the Oregon Dept. of Land Conservation and Development Commission, 24 pp.
KOMAR, P.D.; ALLAN, J.C.; DIAZ-MENDEZ, G.; MARRA, J.J., and RUGGIERO, P., in press. El Niño and La Niña: Erosion processes and impacts. *Proceedings 27th International Conference on Coastal Engineering,* American Society of Civil Engineers.
LEATHERMAN, S.P.; WILLIAMS, A.T., and FISHER, J.S., 1977. Overwash sedimentation associated with a large-scale northeaster. *Marine Geology,* 24, 109–121.
MCKINNEY, B.A., 1976. The spring 1976 erosion of Siletz Spit, Oregon, with an analysis of the causative wave and tide conditions. M.S. Thesis, Oregon State University, Corvallis.
MEI-E, R.; REN-SHUN, Z. and JU-HAI, Y., 1985. Effect of typhoon no. 8114 on coastal morphology and sedimentation of Jiangsu Province, People's Republic of China. *Journal of Coastal Research,* 1, 21–28.
MITCHELL, C.E.; VINCENT, P.; WELDON, R.J., and RICHARDS, M.A., 1994. Present-day vertical deformation of the Cascadia margin, Pacific Northwest, United States. *Journal of Geophysical Research,* 99, 12,257–12,277.
NDBC, 1998. National Data Buoy Center climate data at: http://seaboard.ndbc.noaa.gov/.
NGDC, 1998. National Geophysical Data Center, Worldwide Tsunami Database, Natural hazards data at: http://www.ngdc.noaa.gov/seg/hazard/.
NELSON, A.R.; ATWATER, B.F.; BOBROWSKY, P.T.; BRADLEY, L.-A.; CLAGUE, J.J.; CARVER, G.A.; DARIENZO, M.E.; GRANT, W.C.; KRUEGER, H.W.; SPARKS, R.; STAFFORD, T.W., JR., and STUIVER, M., 1995. Radiocarbon evidence for extensive plate-boundary rupture about 300 years ago at the Cascadia subduction zone. *Nature,* 378, 371–374.
NELSON, A.R.; JENNINGS, A.E., and KASHIMA, K., 1996a. An earthquake history derived from stratigraphic and microfossil evidence of relative sea-level change at Coos Bay, southern coastal Oregon. *Geological Society of America Bulletin,* 108, 141–154.
NELSON, A.R.; SHENNAN, I., and LONG, A.J., 1996b. Identifying coseismic subsidence in tidal-wetland stratigraphic sequences at the Cascadia subduction zone of western North America. *Journal of Geophysical Research,* 101, 6115–6135.
NISHIMURA, Y. and MIYAJI, N., 1996. Investigations of storm deposits caused by a typhoon of September 19th, 1994. *Bulletin of the Natural Disaster Science Data Center Hokkaido,* 10, 15–26.
NOS, 1992. National Ocean Service, Tide gage data at: http:/www.olld.nos.noaa.gov/.
PETERSON, C.D. and DARIENZO, M.E., 1996. Discrimination of climatic, oceanic and tectonic mechanisms of marsh burial, Alsea Bay, Oregon. *In*: ROGERS, A.M.; WALSH, T.J.; KOCKELMAN, W.J., and PRIEST, G. (ed.), *Assessing Earthquake Hazards and Reducing Risk in the Pacific Northwest.* U. S. Geological Survey Professional Paper 1560, pp. 115–146.
PRIEST, G.R., 1995. *Explanation of mapping methods and use of the tsunami hazard maps of the Oregon coast.* Department of Geology and Mineral Industries Open-File Report, Department of Geology and Mineral Industries.
PUGH, D.T., 1987. *Tides, Surges and Mean Sea-Level.* Chichester: John Wiley & Sons, 472p.
REJMÁNIK, M.; SASSER, C.E., and PETERSON, G.W., 1988. Hurricane-induced sediment deposition in a Gulf Coast marsh. *Estuarine, Coastal and Shelf Science,* 27, 217–222.
RUGGIERO, P.; KOMAR, P.D.; MCDOUGAL, W.G., and BEACH, R.A., 1996. Extreme water levels, wave runup and coastal erosion: *Proceedings 25 th International Conference on Coastal Engineering,* American Society of Civil Engineers, p. 2793–2805.
SALLENGER, A.H., 1979. Inverse grading and hydraulic equivalence in grain-flow deposits. *Journal of Sedimentary Petrology,* 49, 2, 553–562.
SATAKE, K.; SHIMAZAKE, K.; TSUJI, Y., and UEDA, K., 1996. Time and size of a giant earthquake in Cascadia inferred from Japanese tsunami records of January 1700. *Nature,* 379, 246–249.
SATO, H.; SHIMAMOTO, T.; TSUTSUMI, A., and KAWAMOTO, E., 1995. Onshore tsunami deposits caused by the 1993 southwest Hokkaido and 1983 Japan Sea earthquakes. *Pure and Applied Geophysics,* 144, 693–717.
SCHWARTZ, R.K., 1975. Nature and genesis of some washover deposits: U.S. Army Corps of Engineers, Coastal Engineering Research Center, *Technical Memoir 61,* pp. 69.
SEYMOUR, R.J., 1996. Wave climate variability in southern California. *Journal of Waterway, Port, Coastal and Ocean Engineering,* American Society of Civil Engineers, 122, 4, 182–186.
SHENNAN, I.; LONG, A.J.; RUTHERFORD, M.M.; INNES, J.B.; GREEN, F.M., and WALKER, K.J., 1998. Tidal marsh stratigraphy, sea-level change and large earthquakes—II: Submergence events during the last 3500 years at Netarts Bay, Oregon, USA. *Quaternary Science Reviews,* 17, 365–393.
SHIH, S.-M. and KOMAR, P.D., 1994. Sediments, beach morphology and sea cliff erosion within an Oregon coast littoral cell. *Journal of Coastal Research,* 10, 144–157.
SHIH, S.-M.; KOMAR, P.D.; TILLOTSON, K.J.; MCDOUGAL, W.G., and RUGGIERO, P., 1994. Wave run-up and sea-cliff erosion: *Proceedings 24 th International Conference on Coastal Engineering,* American Society of Civil Engineers, p. 2170–2184.
STUIVER, M. and REIMER, P.J., 1993. Extended ^{14}C data base and revised Calib 3.0 ^{14}C age calibration program. *Radiocarbon,* 35, 215–230.
TILLOTSON, K.J. and KOMAR, P.D., 1997. The wave climate of the Pacific Northwest (Oregon and Washington): A comparison of data sources. *Journal of Coastal Research,* 13, 440–452.
WILSON, B.W. and TØRUM, A., 1968. The tsunami of the Alaskan earthquake, 1964: Engineering evaluation. *Technical Memorandum No. 25,* Coastal Engineering Research Center, U. S. Army Corps of Engineers, p. 401.
WYRTKI, K., 1975. Fluctuations of the dynamic topography in the Pacific Ocean. *Journal of Physical Oceanography,* 5, 450–459.
ZHANG, K.; DOUGLAS, B.C., and LEATHERMAN, S.P., 1997. East coast storm surges provide unique climate record. *Eos,* 78, 389–397.

APPENDIX A
DIATOM ANALYSES FOR EUCHRE CREEK CORES 2 AND 5

Methods

We cleaned diatom samples with 30% H_2O_2. An aliquot of this solution was transferred to a 22 × 30 mm cover slip and affixed to a glass slide with Naphrax mounting medium. Numbers of brackish-marine species were tallied in 20 vertical traverses of the slide. We estimated the numbers of fresh-brackish diatoms in 20 traverses from the average counted in 5 traverses.

General Paleoecology

Diatom assemblages show that the marsh persisted as a fresh-brackish marsh with episodes of standing water. Most abundant benthic species indicative of a fresh-brackish marsh are species of Eunotia, Gomphonema and Navicula—deposits with greater numbers of *Cyclotella* and *Synedra* reveal periods with standing water, perhaps in small pools on the marsh. An influx of the "Cosmioneis pusilla group" (including Luticola mutica, Pinnularia lagerstedtii, Caloneis bacillum, Navicula cincta, Rhopalodia musculus) in marsh deposits above event 2 on the north side of the marsh (core 5) may indicate slightly more saline conditions nearer a tidal channel.

Table A. 1. *Diatom analyses for Euchre Creek Core 2.*

Core	Gouge core depth (cm)	Lithology	Preservation	Average number of fresh-brackish diatoms per traverse in 5 traverses	Estimated number of fresh-brackish diatoms in 20 traverses	Number of brackish-marine species counted in 20 traverses	Estimated brackish-marine diatoms per 1000 fresh-brackish diatoms
EC95-2	26.5	peaty mud	Good	430	8600		
EC95-2	33	mud	Moderate	357	7140	4.5	0.6
EC95-2	60	mud	Good	1230	24600	3	0.1
EC95-2	61.5	peat	Good	2990	59800	6	0.1
EC95-2	76.5	sand	Poor-Moderate	120	2400	19	7.9
EC95-2	78.5	peat	Poor	770	15400	14	0.9
EC95-2	85	peaty mud	Moderate	1182	23640	2	0.1
EC95-2	89	sand	Moderate-Good	80	1600	7.5	4.7
EC95-2	95	sand	Poor	220	4400	5.5	1.3
EC95-2	101	sand	Poor	251	5020	12.5	2.5
EC95-2	103	peat	Good	960	19200	7.5	0.4
EC95-2	105	sand	Moderate-Poor	440	8800	15.5	1.8
EC95-2	108.5	peat	Good	3100	62000	10.5	0.2
EC95-2	111	sand	Moderate-Poor	42	840	5.5	6.5
EC95-2	125.5	mud	Barren				

Table A. 1. *Extended.*

BRACKISH-MARINE DIATOMS																				
Actinocyclus curvatulus	*Actinoptychus senarius*	*Actinoptychus senarius*	*Actinoptychus splendens*	*Auladiscus probablis*	*Caloneis brevis*	*Chaetoceros* spp. spores	*Cocconeis decipiens*	*Cocconeis scutellum*	*Cocconeis scutellum parva*	*Cosciniodiscus oculus-iridis*	*Cosciniodiscus radiatus*	*Delphineis* cf. *margaritalimbata*	*Delphineis* cf. *surirella*	*Delphineis karstenii*	*Diploneis interrupta*	*Diploneis smithii rhombica*	*Endictya hendeyi*	*Gyrosigma balticum*	*Hemidiscus cuneiformis*	*Melosira moniliformis*
															1					
																			1	
											1				5					
	1							1.5		1							1			
	2					2					1			1	4					
				1							1									
									1	0.5	1				2					
				1							0.5				1					
	2		0.5		1				1		1.5				3.5					
	0.5														2		1			
	1										2		1		3		1.5			
	2							1			1.5			1	1					
				0.5		2									1					

Table A. 1. *Extended.*

BRACKISH-MARINE DIATOMS (extended)																				
Navicula digitoradiata	*Odontella aurita*	*Opephora pacifica*	*Paralia sulcata*	*Rhaphoneis amphiceros*	*Rhaphoneis psammicola*	*silico—Dictyocha fibula*	*silico—Distephanus speculum*	*Stephanopyxis dimorpha*	*Stephanopyxis turris*	*Thalassionema nitzschioides*	*Thalassiosira* cf. *decipiens*	*Thalassiosira* cf. *lineata*	*Thalassiosira eccentrica*	*Thalassiosira lacustris*	*Thalassiosira leptopus*	*Thalassiosira oestrupii*	*Thalassiosira pacifica*	*Thalassiosira simonsenii v. minor*	*Thalassiosira* spp.
			2	0.5													1		
			0.5														1	0.5	
1			4	1	2		1	1		0.5				1			2		
			1	1	1												1		
			1		1							1							
									1		1							1	
				1				1											1
			1										1			1	1		
	1		2	2													1	1	
			1	1								1						1	
				0.5													1.5		

Table A. 1. *Extended.*

BRACKISH-MARINE DIATOMS (extended)				RELATIVE PERCENT OF FRESH-BRACKISH DIATOMS																	
Tryblionella acuminata	*Tryblionella apiculata*	*Tryblionella littoralis*	TOTAL	*Achnanthes* spp.	*Amphora* spp.	*Auliscoseira* spp.	*Cocconeis* spp.	*Cyclotella* spp.	*Cymbella* spp.	*Diadesmis contenta*	*Diploneis* spp.	*Eunotia* spp.	*Fragilaria* spp.	*Frustulia* spp.	*Gomphonema* spp.	*Gyrosigma* spp.	*Hantzschia* spp.	*Mastogloia* spp.	*Melosira* spp.	*Meridion* spp.	*Navicula* spp.
			53	7			1	1	7		1	25			17					1	18
			70.5	12		3	1	2	4			14			29						15
			123	5			1	6	5			1	7		2	1			2		43
			129	8				30	2				27	1	8				6	1	3
1			172	1		1		2			1	12	16		14		2				25
			171	1								43	8		30		1	1			4
						2			3			37	1		42						3
			185.5	1					1			45			45		2				2
			195.5			2		2				26	1		31					1	13
			214.5	1								24	4		33		1				15
			213.5	3				38				2			9						1
			225.5					1	1			30			13						32
			227.5					38					1		10						5
			227.5		1			1		13		6	1		8		16				20

Table A. 1. *Extended.*

RELATIVE PERCENT OF FRESH-BRACKISH DIATOMS (extended)										"Cosmioneis pusilla group"							
Neidium spp.	*Nitzschia* spp.	*Pinnularia* spp.	*Rhoicosphenia* spp.	*Rhopalodia* spp.	*Stauroneis* spp.	*Surirella* spp.	*Synedra* spp.	*Tabellaria* spp.	*Tryblionella* spp.	*Caloneis bacillum*	*Cosmioneis pusilla*	*Diploneis interrupta*	*Epithemia turgida*	*Luticola mutica*	*Navicula cincta*	*Pinnularia lagerstedtii*	*Rhopalodia musculus*	TOTAL %
	11	3			1	3	4											153
1	11				2		2		2		1				1		1	166
	18	2				3	4											220
	3	2				3	7											223
	1	4					2				9.3		2.7	4		2.3		253
	1	3					4	4										257
		4			3		1	4										270
		1			2						1							278
		23			1													290
		21									1							302
	4	7					36											306
	1	9			2						7			4				310
	4	13					30											317
	4	5					2				11			9		4		322

Table A. 2. *Diatom Analyses for Euchre Creek Core 5.*

Core	Depth (cm)	Lithology	Preservation	Average number of fresh-brackish diatoms per traverse in 5 traverses	Estimated number of fresh-brackish diatoms in 20 traverses	Number of brackish-marine species counted in 20 traverses	Estimated brackish-marine diatoms per 1000 fresh-brackish diatoms
EC95-5	37.0	peat	Good	90	1800	1	0.6
EC95-5	43.5	mud	Moderate–Good	37	740		
EC95-5	44.0	mud	Moderate–Good	300	6000	21.5	3.6
EC95-5	46.0	peat	Good	503	10060	48	4.8
EC95-5	66.0	peat	Good	270	5400	20	3.7
EC95-5	81.5	mud	Moderate	770	15400	98	6.4
EC95-5	82.5	sand	Moderate	200	4000	52	13.0
EC95-5	84.0	peat	Poor	25	500	1.5	3.0
EC95-5	105.0	sand	Poor	150	3000	8.5	2.8
EC95-5	115.0	sand	Poor	240	4800	1.5	0.3
EC95-5	122.0	peaty mud	Moderate	1150	23000	6	0.3
EC95-5	123.5	sand	Moderate–Poor	310	6200	58	9.4
EC95-5	124.5	peat	Good	1200	24000	7.5	0.3
EC95-5	125.0	mud	Good	1200	24000	0.5	0.0
EC95-5	126.0	peat	Good	500	10000	4	0.4
EC95-5	133.5	mud	Moderate	110	2200	10	4.5
EC95-5	135.5	sand	Poor	16	320	1.5	4.7
EC95-5	138.5	mud	Barren				

Table A. 2. *Extended.*

BRACKISH-MARINE DIATOMS																					
Actinocyclus curvatulus	*Actinoptychus senarius*	*Actinoptychus senarius*	*Actinoptychus splendens*	*Auladiscus probablis*	*Caloneis brevis*	*Chaetoceros* spp. spores	*Cocconeis decipiens*	*Cocconeis scutellum*	*Cocconeis scutellum parva*	*Coscinodiscus oculus-iridis*	*Coscinodiscus radiatus*	*Delphineis* cf. *marginatalimbata*	*Delphineis* cf. *surirella*	*Delphineis kariostenii*	*Diploneis interrupta*	*Diploneis smithii rhombica*	*Endictya hendeyi*	*Gyrosigma balticum*	*Hemidiscus cuneiformis*	*Melosira moniliformis*
	1	1		2		2									1	2	1			1
	2		1	2.5		3		3			1				6		1			2
1													1		3					
1		8		1		4			13		7				4	2	4	5		3
	1.5				1			2	9	0.5		1			4		3	4		3
											0.5									
			1			2		1						0.5						
								0.5												
				1																
	2	1				3		2	1		1		1	1			2			
				1						0.5	1			1	1					
				2							0.5				0.5					
	0.5													1	5		1			
							1													

Table A. 2. *Extended.*

BRACKISH-MARINE DIATOMS (extended)																				
Navicula digitoradiata	*Odontella aurita*	*Opephora pacifica*	*Paralia sulcata*	*Rhaphoneis amphiceros*	*Rhaphoneis psammicola*	*silico—Dictyocha fibula*	*silico—Distephanus speculum*	*Stephanopyxis dimorpha*	*Stephanopyxis turris*	*Thalassionema nitzschioides*	*Thalassiosira* cf. *decipiens*	*Thalassiosira* cf. *lineata*	*Thalassiosira eccentrica*	*Thalassiosira lacustris*	*Thalassiosira leptopus*	*Thalassiosira oestrupii*	*Thalassiosira pacifica*	*Thalassiosira simonsenii* v. *minor*	*Thalassiosira* spp.
	1																		
			3											1			5		
	3		1	1		2				1	3		1		0.5		14		
		1	5								2		1				6		
1	5		6	1.5	1		8			0.5			4	3	1		13		1
			5		2		1			0.5				4	0.5		7.5		2
			1																
1				1						1							1		
																	1		
							2										2	1	
				1	2		1			3			0.5				34	1	1.5
			1														1	1	
																	0.5		
																	1		
			2												0.5				
			0.5																

Table A. 2. *Extended.*

BRACKISH-MARINE DIATOMS (extended)				RELATIVE PERCENT OF FRESH-BRACKISH DIATOMS															
Trybli-onella acumi-nata	*Trybli-onella apicula-ta*	*Trybli-onella littoral-is*	TOTAL	*Achnan-thes* spp.	*Ampho-ra* spp.	*Aula-cos-eira* spp.	*Cocco-neis* spp.	*Cyclo-tella* spp.	*Cymbel-la* spp.	*Diades-mis con-tenta*	*Diplo-neis* spp.	*Eunotia* spp.	*Fragi-laria* spp.	*Frustu-lia* spp.	*Gom-pho-nema* spp.	*Gyro-sigma* spp.	*Hantz-schia* spp.	*Masto-gloia* spp.	*Melosi-ra* spp.
			75	3			1	2	5			2		5	20	1			
			87	8			4	2			1	1	1	3	10	1			
1.5	1		110.5	2				2			2			6	6			2	
			140	3			1	16	2				5		8				2
			152	7	1			2	4		3	4	10		2				
1		1	262	1									5	4	9				
0.5			217			2		2			1	1	33		7				2
			169.5	1		7			1			22	3	2	23				2
			218.5					3	1			9	3		25				
			231.5			3		10	3		1	9	20		29				
			250					26					17		7				
			305			12	2	4				14	15		28				
			256.5			6		2				26	14		34				
			250.5			35			2			4	36		15				
			256			16		1	2			13	31		15				
			277	1		7	1	6	1	1		1			12		1.5		
			272.5	1		5	3			2		16	4		26		2		
												3			3		1		

Table A. 2. *Extended.*

RELATIVE PERCENT OF FRESH-BRACKISH DIATOMS (extended)												"Cosmioneis pusilla group"								
Meri-dion spp.	*Navicu-la* spp.	*Nei-dium* spp.	*Nitz-schia* spp.	*Pinnu-laria* spp.	*Rhoi-cos-phenia* spp.	*Rhopa-lodia* spp.	*Stau-roneis* spp.	*Surirel-la* spp.	*Syne-dra* spp.	*Tabel-laria* spp.	*Trybli-onella* spp.	*Calo-neis bacil-lum*	*Cosmi-oneis pusilla*	*Diplo-neis inter-rupta*	*Epi-themia turgida*	*Luti-cola mutica*	*Navicu-la cincta*	*Pinnu-laria lager-stedtii*	*Rhopa-lodia mus-culus*	TOTAL %
	23		22	4	1				8			2	1							100
	12		26	3	4			6	5		1		7					5		100
	21		16					4	2			4	17			2	2	12		100
	16		14	8	4		2				4		6					9		100
	19		14	7			2				2	6	10			2	2	3		100
	45		8						2		1		11			12		2		100
	28		9			1			5	1	1		1			2	1	3		100
	13		7	11		1	1		4							2				100
			14				4		40		1									100
	2		8	2			2		8	3										100
			3	5		6	4		32											100
	8		7	4			4		2										1	100
	3			13			2													100
			3	3					1						1					100
	6		2	1			2		10	1										100
	228		2.5	2			5		19				7		2	1				100
	5		5	9			6		5	1			2			5	2	1		100
	2		2	2																